

To appear in *The Astronomical Journal*

The variable star population in Phoenix: coexistence of Anomalous and short-period Classical Cepheids, and detection of RR Lyrae variables.

C. Gallart¹ and A. Aparicio

Instituto de Astrofísica de Canarias. 38200 La Laguna. Tenerife, Canary Islands. Spain.

carme@iac.es, aaj@iac.es

W.L. Freedman

Observatories of the Carnegie Institution of Washington. 813 Santa Barbara St. Pasadena CA 91101, USA

wendy@ociw.edu

B.F. Madore

NASA Extragalactic Database, Infrared Processing and Analysis Center, California Institute of Technology, MS 100-22, Pasadena, CA 91125, USA

barry@ipac.caltech.edu

D. Martínez-Delgado

Max Planck Institute for Astronomy, Königstuhl 17, D69117 Heidelberg, Germany

ddelgado@mpia-hd.mpg.de

and

P.B. Stetson

Herzberg Institute of Astrophysics, National Research Council, Victoria, BC, Canada V9E 2E7

Peter.Stetson@nrc.gc.ca

¹Ramon y Cajal Fellow. Instituto de Astrofísica de Canarias. 38200 La Laguna. Tenerife. Spain.

ABSTRACT

We present the results of a search for variable stars in the Local Group dwarf galaxy Phoenix. Nineteen Cepheids, six candidate long-period variables, one candidate eclipsing binary and a large number of candidate RR Lyrae stars have been identified. Periods and light curves have been obtained for all the Cepheid variables. Their distribution in the period–luminosity diagram reveals that both Anomalous Cepheids (AC) and short-period Classical Cepheids (s-pCC) are found in our sample. This is the first time that both types of variable star are identified in the same system even though they likely coexist, but have gone unnoticed so far, in other low-metallicity galaxies like Leo A and Sextans A. We argue that the conditions for the existence of both types of variable star in the same galaxy are a low metallicity at all ages, and the presence of both young and intermediate-age (or old, depending on the nature of AC) stars. The RR Lyrae candidates trace, together with the well developed horizontal branch, the existence of an important old population in Phoenix. The different spatial distributions of s-pCC, AC and RR Lyrae variables in the Phoenix field are consistent with the stellar population gradients found in Phoenix, in the sense that the younger population is concentrated in the central part of the galaxy. The gradients in the distribution of the young population within the central part of Phoenix, which seem to indicate a propagation of the recent star formation, are also reflected in the spatial distribution of the s-pCC.

Subject headings: galaxies: Local Group; galaxies: individual: Phoenix; variable stars: Cepheids; variable stars: RR Lyrae

1. Introduction

Variable-star studies are experiencing a spectacular resurgence thanks to the microlensing projects which, as a by-product, are supplying huge samples of variable stars, mainly in the LMC, SMC and the Galactic Bulge. On another hand, HST and many ground-based sites with excellent seeing are allowing us to probe deep into the stellar populations of Local Group dwarf irregular (dIrr) galaxies, thus providing information on variable stars only observable before in the dwarf-galaxy satellites of the Milky Way. These enlarged samples of variable stars of different types provide the necessary information to deepen our understanding of the characteristics of each type, the relationships between them, and the physical mechanisms involved in their light variation, which yield important tests of stellar evolution

models. At the same time, the gathering of data in different galaxy environments makes it possible to relate the types of variable stars to the stellar populations in their host galaxies.

These studies have provided, in particular, relatively large samples of short-period Classical Cepheids (s-pCC) in a number of dIrr galaxies: the SMC (Bauer et al. 1999; Udalski et al. 1999), IC1613 (Dolphin et al. 2001), Leo A (Dolphin et al. 2002) and Sextans A (Dolphin et al. 2003). As pointed out by Gallart et al. (1999) and Dolphin et al. (2002), short-period ($P \simeq 1$ day) variables, with Cepheid-like light curves and luminosities about 1 magnitude above the horizontal branch can be produced by young¹ stars in the phase of core He burning which, in the case of low-metallicity stars, experience blue loops extended enough to the blue to cross the instability strip. The so-called Anomalous Cepheids (AC) and s-pCC lie in similar positions in both the color–magnitude and the period–luminosity (PL) diagrams, and they are found in basically every dwarf Spheroidal (dSph) galaxy that has been surveyed for them, as well as in one globular cluster (Pritzl et al. 2002; and references therein). The term “Anomalous Cepheid” was first introduced by Norris & Zinn (1975) because they are more luminous at a given period than the Population II Cepheids found in globular clusters. AC are $\simeq 0.5$ –2 magnitudes brighter than RR Lyrae stars, and their periods range from 0.3 to 2 days. Concerning their evolutionary status, there is general agreement that they are metal-poor stars with mass $\simeq 1.5M_{\odot}$, occupying the instability strip during their horizontal-branch phase of evolution (Demarque & Hirshfeld 1975; Hirshfeld 1980; Bono et al. 1997). They may be either i) evolved, single, intermediate-age (≤ 5 Gyr) stars, or ii) the evolved products of mass transfer in old ($\simeq 12$ Gyr) binary systems. The predicted behaviour in both cases is very similar (Bono et al. 1997), and it has therefore been considered impossible to distinguish between the two possible origins of AC from their location in the PL and color-magnitude diagrams alone (Nemec, Nemec & Lutz 1994 and Dolphin et al. 2002).

A reanalysis of all the data accumulated to date on AC by Bono et al. (1997) and Pritzl et al. (2002) provided a slightly different locus for the AC in the PL diagram that, as we will show in the present paper, may allow one to discriminate these two types of variable star. Since they respectively trace stellar populations of different ages and of a very specific metallicity range, this distinction is relevant to the use of variable stars as bright tracers of stellar populations of different ages (in this case, AC as tracers of a fainter intermediate-age or old population), and as anchors of the age–metallicity relation of individual dwarf galaxies.

Prior to this study, AC and s-pCC have not been identified in the same galaxy. As

¹Throughout the paper, we will consider as young populations those stars younger than 1 Gyr, while intermediate-age populations will be defined broadly as those having ages of 1–10 Gyr

mentioned above, AC are routinely found in dSph galaxies while s-pCC have been found in dIrr galaxies. Since both types of variable star have very similar characteristics, it may be that the classification of some of them has been prejudiced by the type of galaxy in which they were found. A suitable type of object in which to search for *both* types of variable are the so-called transition-type dSph/dIrr galaxies (Mateo 1998). The closest such system is Phoenix. We had started a search for variable stars in this galaxy, and along the way we realized that it was, in fact, an ideal system to address this problem.

Phoenix is a low-mass ($M_{tot} = 3.3 \times 10^6 M_{\odot}$), low-metallicity ($[Fe/H] = -1.4$) system at a distance of about 400 Kpc $[(m - M)_{\odot} = 23.0 \pm 0.1]$ from the Milky Way (Mateo 1998; Martínez-Delgado, Gallart & Aparicio 1999, MGA99 hereinafter; Held, Saviane & Momany 1999; and references therein). The fact that it has a small young stellar population (up to about 100 Myr old), embedded in a substantial population of old and intermediate-age stars (MGA99; Held et al. 1999) and little or no gas (St-Germain et al. 1999; Gallart et al. 2001) has motivated its classification as a transition type dSph/dIrr galaxy. No studies of variable stars in Phoenix have been published to date, although some suspected variable stars were reported by van de Rydt, Demers & Kunkel (1991) and MGA99. Both its low metallicity and the existence of stars of all ages made it a good candidate to search for both AC and s-pCC. In this paper we report such a discovery. We also discuss the possible existence of both types of variable star in other dwarf galaxies and the information that they may provide on the age-metallicity relations of their host galaxies. We also report, for the first time, the discovery of a large number of RR Lyrae variable star candidates in Phoenix which trace, together with the well developed horizontal branch, the existence and distribution of an old population in the galaxy.

2. Observations and data reduction

Phoenix was observed in 1997, 2000, and 2001 during four approximately week-long runs using the 2.5m duPont telescope at Las Campanas Observatory. In addition, we included one epoch obtained by ourselves with FORS1 at the VLT and several epochs of ESO archival data obtained with either the NTT (with EMMI or SUSI) or the VLT. Since our initial goal was the study of the Cepheid population in Phoenix, we typically performed observations once per night in two bands (V and either B or I) during each of the Las Campanas runs, except on the first run, when several images per night were obtained for the stellar-populations study published by MGA99. All the observations available to us are listed in Table 1. Only images with seeing better than $1''.5$ were used for the present study.

The images were processed in the standard way using IRAF to apply bias and flat-field

frames obtained on the corresponding nights. Profile-fitting photometry was obtained using the DAOPHOT/ALLSTAR/ALLFRAME suite of programs (Stetson 1987; Stetson 1994). A master frame for Phoenix was created from the median of 60 B , V and I LCO images with $\text{FWHM} \leq 4$ pix (i.e., seeing $\leq 1''$). Geometric transformations between frames, including cubic distortions in addition to translations and scale changes, were calculated using DAOMASTER (Stetson 1990). MONTAGE2 was used to create the medianed image, which was then searched for stars. A total of $\simeq 14,700$ stars were found and input to ALLFRAME, to be photometered on a total of 19 B , 48 V , and 45 I good-seeing ($\leq 1''.5$) images. Mean B , V , and I magnitudes at each epoch were obtained for each star in the corresponding set of images in each filter, again using DAOMASTER. Aperture corrections were obtained from a large number of isolated stars in one image for each of B , V , and I . These are estimated to be accurate to ± 0.003 mag in B , ± 0.008 mag in V , and ± 0.006 mag in I . Photometric transformations to the Johnson-Cousins standard system of Landolt (1992) were obtained using standard-star measurements in two of the observing runs.

In February 1997, we obtained approximately 140 measurements of Landolt standard stars in V and $\simeq 120$ in I , providing a good sampling at all airmasses up to $X \simeq 2.0$. They were used to obtain atmospheric and instrumental coefficients for transforming our instrumental magnitudes to the Johnson V and Cousins I standard photometric systems. These same stars were used to obtain the instrumental coefficients published in MGA99, but a later reanalysis of the same data showed that an error had been made in the sign of one of the color terms. The corrected equations used to transform our instrumental magnitudes into the Johnson-Cousins system are:

$$V - v = 24.766 - 0.029(V - I) \quad (1)$$

$$I - i = 24.443 + 0.032(V - I) \quad (2)$$

The photometric conditions during the campaign were stable and produced very small zero-point errors for the photometric transformations: ± 0.006 mag in V and ± 0.009 mag in I . The standard errors in the extinction were always smaller than 0.012 in both V and I . Taking all the uncertainties into account, we estimate a total error in the photometry zero point of 0.02 mag in both V and I .

The most important difference between these equations and those listed by MGA99 is in the sign of the color term of equation (2) (we also find a different numerical value for the zero point, but this is mostly compensated by a corresponding change in the calculated extinction coefficients). With this new color term, the discrepancy in the color of the RGB tip between MGA99 and both van de Rydt et al. (1991) and Held et al. (1999) — which was

acknowledged by MGA99 — has disappeared.

The B transformations were determined from 10 observations of 3 Landolt (1992) standard stars in the December 2001 observing run. The corresponding transformation equation is:

$$B - b = 24.547 + 0.043(B - V) \quad (3)$$

The total uncertainty in the B zero-point (extinction, photometric transformation, and aperture correction) is estimated to be ± 0.02 .

Figure 1 shows the $[(B-V), V]$ and $[(V-I), I]$ CMDs obtained by combining all the data. Note that a blue-extended, well populated horizontal branch (HB), which was hinted in both MGA99 and Held et al. (1999), shows up beautifully in both CMDs. An RR Lyrae gap also clearly appears in both diagrams.

3. Selection of candidate variable stars

We made a first selection of candidate variable stars based on both the variability index var , defined as the ratio of the external (σ_{ext}) to the internal (σ_{int}) standard error², and on the external standard error of one measurement (σ_{ext}) itself, as calculated by DAOMASTER from the individual magnitudes of the 48 V images we ultimately used. The stars with $var \geq 2.0$ and $\sigma_{ext} \geq 0.05$ were flagged as candidate variable stars. The second requirement was set in order to discard many bright stars whose large variability index originated in a very small internal standard error (which is itself a derived statistic subject to observational noise and round-off error), and thus were not *bona fide* candidate variable stars. Also, the area corresponding to the brightest star in the field was masked, since the star image was generally saturated. These requirements produced a list with about 800 variable-star candidates. These candidates were then individually examined using the image display to

²The *internal* standard error of the magnitude measured for a single star in a single image, σ_{int} , is estimated from the known readout noise of the detector and the Poisson photon noise of star and sky as scaled by the known gain of the detector, and also from the pixel-to-pixel agreement between the observed stellar profile and the shifted and scaled point-spread function for the image. The *external* standard error per observation for a given star, σ_{ext} , is derived from the frame-to-frame agreement between its individual magnitude measurements. A star that is actually varying in luminosity and that has been well measured at most or all epochs should have $var \equiv \sigma_{ext}/\langle\sigma_{int}\rangle \gg 1$, where $\langle\sigma_{int}\rangle$ is a suitable estimate of the “typical” internal error for the star. This index cannot be justified with full mathematical rigor; nevertheless, it is apparent that that minority of stars having stand-out values of var are the most likely to be genuine variables.

discard problematic stars: any candidate i) in the wings of a companion star or galaxy much brighter than itself, or ii) with a companion star that ALLFRAME failed to separate, or iii) with poorly subtracted neighbors. In this way, about 25% of the candidates were discarded. Even though some of these criteria may discard *bona fide* variable stars, they would be stars with poorly determined magnitudes or with magnitude errors likely to be sensitive to the seeing, for which accurate periods would be difficult to determine. This left a list of $\simeq 590$ stars; these remaining candidates are represented in Figure 2. Note that the fact that there are many candidates among the brightest blue and red stars, where they are not *a priori* expected, indicates that some of them will still be spurious³.

Subsequently, these 590 candidate variable stars were divided into two groups: those above the HB, *i.e.*, brighter than $V \simeq 23.2$ which would be Cepheid, eclipsing or long-period variable candidates, and those fainter, which are RR Lyrae variable-star candidates. No candidates were discarded *a priori* based on their color, since we are interested in all kinds of variable stars, and not only pulsating variable stars in the instability strip. In addition, the *mean* magnitudes computed at this point were just straight averages of all data points (weighted by the photometric errors), and not properly intensity-averaged, phase-weighted magnitudes. The colors computed from them, therefore, may be affected by a different sampling of the the light curve in the two bands, and therefore substantially different from actual mean colors⁴. This, in fact, appears to be the case for two of the *bona fide* pulsating variables discovered, which had very blue inferred ($B-V$) colors (see below).

3.1. The bright candidates

The selection described above produced a list of 202 *bright* ($V \leq 23.2$) candidates. The light variation of these stars over all epochs was examined graphically and compared with

³These spurious candidates still originate in stars that have very small internal errors σ_{int} resulting in large values of the *var* index, which indicates that the condition $\sigma_{ext} \geq 0.05$ has not been stringent enough. We preferred, however, to retain these stars and search for variability on them, rather than risk discarding possible *bona fide* low-amplitude variables.

⁴Note however, that the color terms in the photometric transformations are small (0.03–0.04 mag), so that even if the colors are wrong by 1.0 magnitudes, the individual calibrated magnitudes would still only be off by 0.03–0.04 mag due to the incorrect inferred colors. In addition, one iteration in the calculation of the individual calibrated magnitudes was performed: in a first pass, the straight average B , V and I magnitudes were used to calculate the colors of each star to be used in transforming the instrumental magnitudes to standard magnitudes using eqs. (1–3). Subsequently, intensity-averaged, phase-weighted magnitudes were calculated for each star, and used in a refined transformation of the individual-epoch magnitudes.

the magnitude scatter of non-variable stars of similar magnitude. In the process, a large fraction of candidates was discarded because their light variations were similar to the average magnitude dispersion at the corresponding magnitude. From the characteristics of the light variation, 47 candidates seemed periodic, 17 were candidate eclipsing binaries, and 9 were candidate long-period variables. All eclipsing binary candidates but one were discarded after examination of the star image in the frame that corresponded to minimum light, in most cases because it was on a bad column of the detector. Among the long-period variable candidates, however, 6 are likely legitimate variable stars.

The light variations of all the candidate pulsating “bright” variables (likely s-pCC or AC) were searched for periodicities. We used the three following methods: i) the Stellingwerf (1978) phase dispersion minimization algorithm; ii) our own modified string-length algorithm, which considers the data from all filters simultaneously and takes into account the photometric uncertainty associated with each data point; and iii) the routines created by Andy Layden (Layden 1998; Layden & Sarajedini 2000), which determine the most likely period by fitting the photometry of the variable star with 10 templates over a selected range of periods. For methods i) and iii) we used only the V data points. In most cases, the same best period was found by all three methods. In only a few cases, one of the three methods produced a period that the other methods didn’t find, and which turned out to be the best upon examination of the light curves.

We visually inspected the light curves that each of the most likely periods would produce for each variable, in *all three* bands. When more than one likely period was found, the quality of the derived light curve was used to decide among them. In a few cases, more than one period produced acceptable light curves. In these cases, we used the position in the period-luminosity (PL) diagram (see Section 5) to identify the most likely periods (see Table 2).

For 15 candidates, clear periods were found, while 4 have uncertain periods. The periods are all shorter than 2 days, and about half of the variables have periods shorter than 1 day. The PL distribution of the Phoenix variables will be discussed in Section 7, together with the nature of these variable stars. In Table 2 the identification of each variable, its period, the phase-weighted intensity-averaged magnitude (Saha & Hoessel 1990) in each band, and its most likely sub-class are listed. The intensity-averaged magnitudes (not phase-weighted) were also calculated for all these variables. The differences from the phase-weighted magnitudes are of a couple of tenths of a magnitude at most. The phase-weighted magnitudes produce tighter sequences in the CMD and are preferred as a best representation of the true mean magnitude. The BVI light curves for these stars are displayed in Figure 3.

The final list of confirmed pulsating and long-period variables, and the one candidate eclipsing binary star are listed in Table 2. A finding chart is displayed in Figure 4. The B ,

V , and I photometry of the variables at the different epochs is listed in Tables 3, 4 and 5 respectively. They are shown in Figure 5, together with all the candidate RR Lyrae variable stars (see Section 3.2).

3.2. The RR Lyrae candidates

The RR Lyrae candidates are close to the photometric limit of our CMD, and in most cases, their light variations are similar to the photometric errors expected at the corresponding magnitude level. For most of them no definite period can be assigned, and an exhaustive search has not been performed. The great concentration of candidate variable stars in the HB (see Figure 2), with almost no variable stars with redder or bluer colors at similar magnitudes, however, supports the idea that we are indeed detecting the light variations of RR Lyrae variables. A few light curves for RR Lyrae for which clear periods have been found are shown in Figure 6.

4. Nature of the Cepheid variables in Phoenix: Classical or Anomalous?

In Figure 7 the PL diagrams for the Phoenix Cepheids in the B and V bands are represented. A distance modulus $(m - M)_0 = 23.1$ and a reddening $E(B - V) = 0.02$ (Held et al. 1999) have been assumed. Because the number of Cepheid variables found in this work is relatively small (as expected in a low-mass system with little current star formation), we prefer to use the tip of the RGB as a robust distance indicator rather than trying to derive a distance from the variables themselves. Given this value for the true distance modulus, the pulsating variables located above the horizontal branch extend from $M_V \simeq -2$, $M_B \simeq -1.8$ down to $M_V \simeq 0$ and $M_B \simeq 0.3$, virtually merging with the RR Lyrae locus, and forming therefore a continuum in the instability strip.

To further constrain the nature of these variables from their positions in the PL plane, the PL relations obtained by fitting the s-pCC in the OGLE database, and the PL relations obtained by Pritzl et al. (2002) for Local Group dSph AC have been overplotted on the Phoenix data in Figure 7.

Because of the change in the PL relation slope at a period of about 2 days (Bauer et al. 1999; the effect is also clearly visible in the OGLE SMC Cepheids), we fit a PL relation for s-pCC in the OGLE SMC database. Assuming a SMC distance modulus of $(m - M)_0 = 18.66$ and mean reddening $E(B - V) = 0.09$ (Udalski et al. 1999), the PL relations become:

$$M_{B,FM} = -2.66(\pm 0.12)\log(P) - 0.92(\pm 0.02) \quad (4)$$

$$M_{B,FO} = -3.24(\pm 0.06)\log(P) - 1.58(\pm 0.01) \quad (5)$$

$$M_{V,FM} = -3.08(\pm 0.10)\log(P) - 1.12(\pm 0.02) \quad (6)$$

$$M_{V,FO} = -3.31(\pm 0.06)\log(P) - 1.78(\pm 0.01) \quad (7)$$

As discussed by Dolphin et al (2002), these relations are virtually identical to the PL relations for AC obtained by Nemec et al. (1994)⁵. In contrast, the PL relations for AC obtained by Pritzl et al. (2002) are substantially different:

$$M_{B,FM} = -2.62(\pm 0.18)\log(P) - 0.40(\pm 0.04) \quad (8)$$

$$M_{B,FO} = -3.99(\pm 0.27)\log(P) - 1.43(\pm 0.09) \quad (9)$$

$$M_{V,FM} = -2.64(\pm 0.17)\log(P) - 0.71(\pm 0.03) \quad (10)$$

$$M_{V,FO} = -3.74(\pm 0.20)\log(P) - 1.61(\pm 0.07) \quad (11)$$

The dataset on which Pritzl et al. (2002) based their fit to the AC PL relation is somewhat larger than the dataset available to Nemec et al. (1994), and shows clearly the different slope of the fundamental mode and first overtone relations, of which there was already a hint in the work of Nemec et al. (who decided, nevertheless, to keep the two relations parallel in view of the lack of clear statistical evidence for different slopes). We will use the Pritzl et al. relation for AC, which is also very similar to the Bono et al. (1997) relation, in the remainder of this paper.

In Figure 7, there is some evidence that we find both types of Cepheid in Phoenix. Down to $M_V \simeq -1$, the variables seem to follow the SMC s-pCC PL relation quite nicely, while at fainter magnitudes they follow the AC PL relation much better. In the remainder of the paper, we will adopt this limit to assign each of the Phoenix Cepheid variables to one of the two subtypes (Table 2, and Figure 9). This is the first time that the two types of Cepheid have been identified in the same system. Previously, AC were clearly identified only in dSph galaxies and globular clusters, while s-pCC were identified in several dIrr galaxies (see Section 6). It is fortuitous that the first identification of both AC and s-pCC has occurred in a galaxy of the so-called dSph/dIrr transition type (Mateo 1998). We will discuss in

⁵Nemec et al. (1994) give a PL relation for AC which depends on metallicity. Their relation is closest to the PL relation for s-pCC at the lowest possible metallicities, while it departs substantially from the s-pCC under the assumption of a higher metallicity

Section 6 that both kinds of variables may have been observed in other galaxies considered pure dIrr systems, even though the presence of AC went unnoticed.

5. Spatial distribution of stellar populations

Because AC and s-pCC are representatives of stellar populations of different ages (basically, older and younger than 1 Gyr, respectively) we may expect that, if our interpretation of the nature of the variables in Phoenix is correct, they must show different distributions consistent with the stellar population gradients that have already been noted in Phoenix. MGA99 showed that all the young stars in Phoenix are concentrated in a flattened inner component with a maximum extent of ≈ 458 pc (approximately $4'$) east-west, while the older stars extend farther out (diameter > 900 pc $\simeq 7'.8$) as a somewhat flattened component oriented North–South. In the inner, young component, a gradient in the age of the stars is observed, with the youngest stars ($\simeq 100$ Myr old) predominantly located in its western half, and likely remnants of gas lost by the galaxy after this last event of star formation situated $6'$ southwest from the center of the galaxy (Gallart et al. 2001).

To show that the variable stars are correlated as expected with the rest of the stellar populations in Phoenix, a few isochrones have been plotted in the Phoenix CMD (see Figure 8). Candidate s-pCC stars are represented as circles and AC as stars (using, as defined in Section ref, $M_V = -1$ as the cutoff magnitude between them). The s-pCC variables are well matched by the blue loops of low-metallicity ($Z = 0.001 - 0.0004$), 400–600 Myr old stars. Stars of the same age are also found in the main sequence of the same CMDs. As calculated by Gallart et al. (1999), a star of this age in the blue-loop phase would have an expected period $P \simeq 1.2$ days, which is in the middle of the period range found for these s-pCC. The ACs are well matched by the ”hooks” (Bono 2003) of He-burning 1–2 Gyr old, very metal-poor ($Z = 0.0001$) stars.

In Figure 9 we have plotted the positions of the variable stars of different types in Phoenix. The s-pCC variable stars (marked as circles in Figure 9), are concentrated in the central part of the galaxy where the most recent star formation has taken place. They also show a very flattened distribution, oriented in the same direction as the young Phoenix component. The AC variable stars (marked as stars in Figure 9) are much more widely distributed, as is the intermediate-age population in Phoenix. The RR Lyrae candidates are even more widely distributed, and they probably trace the true extension of the old population in Phoenix which, as concluded by MGA99, seems to have a spheroidal distribution extending farther than the younger inner component.

Because the AC variables in Phoenix are appreciably less widely distributed on the sky than the RR Lyrae candidates, throughout the rest of this paper we will tacitly assume that the AC variable stars in Phoenix have evolved from single intermediate-age stars (age \sim a few Gyr) rather than from mass-exchange binaries in an old (~ 10 Gyr) population. We admit that this assertion is not yet decisively proven; AC of both types of provenance could well exist in Phoenix or other systems.

Going back in more detail to the spatial distribution of the bright s-pCC variables, it is interesting that most of them are located preferentially in the eastern half of the Phoenix central zone, opposite to the locus of the very youngest population. In principle, one might have expected some brighter, slightly longer-period variables in the western part of the galaxy, but these are not found. From Figure 8, it can be seen that the population in the western part is as young as 100 Myr. As discussed by Dolphin et al. (2001), the bright blue loops are less strongly populated than the fainter ones, and small-number statistics may be the reason for not finding younger Cepheids. All this is consistent with the hypothesis of a propagation of the star formation in the central component of Phoenix as put forward by MGA99: a burst of star formation would have started $\simeq 600$ Myr ago in the eastern part, where most of the variables of that age are found, and propagated westward, where it was active just $\simeq 100$ Myr ago.

Finally, in Figure 10, RGB, RR Lyrae and Cepheid star counts over several radial bins are displayed. Note the different distribution as a function of radius of RGB stars and RR Lyrae candidates: the RGB stars are substantially more centrally concentrated than the RR Lyrae candidates, whose distribution out to $\simeq 70$ arcsec from the center of the galaxy is relatively flat (inside this radius, completeness effects may play a role), and certainly flatter than that of the RGB stars. This may indicate that the old population of the galaxy, traced by the RR Lyrae candidates, is more uniformly distributed than the RGB, which is likely a mixture of old and intermediate-age populations (in the central $3'$ of the galaxy at least). A detailed discussion of the radial distribution of stellar populations of different ages in Phoenix, using HST data, will be presented by Hidalgo, Aparicio & Martínez-Delgado 2003, in prep).

6. Discussion: Anomalous *vs.* short period Classical Cepheids: why are they rarely found in the same system?

From a stellar-evolution point of view, both AC and s-pCC are central He-burners, the difference between them being the fact that the AC started the core He burning under degenerate conditions (Bono et al. 1997), whereas s-pCC are stars massive enough to have

ignited He in the core under non-degenerate conditions. The former are, therefore, older than the latter, as discussed in the Introduction. As was also discussed and demonstrated by Dolphin et al. (2002), the reason for the existence of large numbers of s-pCC in low-metallicity systems is that the blue loops extend farther to the blue for stars of lower metal abundance and, as a consequence, the shorter but more populated blue loops of relatively low-mass, old stars may enter the instability strip. Because the "hooks" of intermediate-age He-burning stars also reach the instability strip only in the case of low metallicity (Bono 1997), both AC and s-pCC can exist only in low-metallicity systems, and the existence of one or the other depends on the stars of the appropriate age being present in the galaxy. Both types of variables coexist in Phoenix probably thanks to its very low metallicity and the presence of stellar populations of all ages.

In some of the dSph satellites of the Milky Way, the relatively short-period variable stars situated above the horizontal branch must necessarily be AC, since no other stars young enough to produce blue loops are observed in them. In others — like Leo I — there is a low-metallicity population young enough to potentially provide s-pCC (Gallart et al. 1999). On the other hand, no AC have been identified so far in dIrr galaxies. Part of the reason may be that dIrr are too distant for stars of such low luminosity to be detected. On the basis of limiting magnitude they could have been detected, however, in the SMC and LMC, and in IC1613, Leo A, and Sextans A (specifically, in the recent studies by Dolphin et al. 2001, 2002, 2003). In the SMC OGLE database, for example, a comparatively small number of objects fall along the AC PL relation obtained by Pritzl et al. (2002; see also Smith et al. 1992). The reason for the lack of clear AC sequences in the LMC and SMC may be that their metallicities are too high.

In the case of Leo A, Dolphin et al. (2002) concluded that all their variables are compatible with being s-pCC and that, in any case, these could not be distinguished from AC on the basis of their position in the PL plane. (Note that they were considering the Nemec et al. PL relation for AC of very low metallicity, which is basically identical to that of s-pCC.) Since Leo A is supposed to be a very low-metallicity galaxy like Phoenix, and does contain an old population as evidenced by the presence of a number of RR Lyrae stars (Dolphin et al. 2002), one would expect that AC could also exist in it. In the following we will show that, in fact, the distribution of Cepheids in the Leo A PL diagram is better fit if both AC and s-pCC PL relations are assumed to be present, as opposed to only s-pCC as assumed by Dolphin et al. (2002). In Figure 11, Figure 8 of Dolphin et al. (2002) is reproduced, but the Pritzl et al. (2002) AC PL relation has been superimposed. Note that a number of stars situated below the PL relations of both fundamental-mode and first-overtone s-pCC are nicely fit by the AC PL relations. We think, therefore, that both types of variables are present in Leo A as well as in Phoenix. A similar situation occurs in Sextans A (see Figure 11), even

though very few variable stars have been detected in this galaxy below $M_V = -1$, and thus the main magnitude range occupied by AC is missing.

We conclude, therefore, that the only requirements for the coexistence of s-pCC and AC in a given galaxy is that its metallicity be low enough ($Z \simeq 0.0004$) and that there have been star-formation activity at all ages. The two populations of variables can be distinguished in the PL plane and their presence or lack thereof can provide important hints about the age–metallicity relation of the host galaxy.

According to the metallicity–absolute magnitude relation observed for dwarf galaxies, which implies that low-luminosity systems are also metal-poor, we expect to find both AC and s-pCC in the smallest dIrr galaxies, e.g. NGC6822 (see Clementini et al. 2003), IC1613, Leo A, Sextans A, Sextans B, Pegasus, LGS3, and Antlia.

Finally, Mateo, Fischer & Krzemiński (1995) examined the specific frequency S of ACs (number of AC per $10^5 L_{V,\odot}$) in dSph galaxies and found a good correlation between S and galaxy magnitude. Pritzl et al. (2003) updated this relation with all the currently available data. It is interesting to check whether galaxy types other than dSph follow the same relation. In the case of Phoenix, with 11 AC and a luminosity of $9 \times 10^5 M_\odot$, $S = 1.2$, which is almost exactly what one would expect from the Pritzl et al. (2003) relations — $\log S$ both as a function of absolute magnitude and as a function of $[\text{Fe}/\text{H}]$.

7. Summary and conclusions

A search for variable stars has been conducted in the Phoenix dwarf galaxy. Nineteen Cepheids (either AC or s-pCC), six candidate long-period variables, one candidate eclipsing binary and a large number of candidate RR Lyrae stars have been identified. Periods and light curves have been obtained for all the Cepheid variables. Their distribution in the PL diagram reveals that both AC and s-pCC are present in our sample. This is the first time that both types of variable star, which belong to metal-poor old/intermediate-age and metal-poor young populations respectively, have been identified in the same system. We show, however, that they also likely coexist in Leo A and Sextans A, even though the fact originally went unnoticed. We note that, thanks to the very specific conditions of age and metallicity required for the occurrence of these variables, they can provide important hints on the age–metallicity relation of the host galaxy. For example, in the case of Phoenix they imply, according to current stellar-evolution models, a very low metallicity ($Z = 0.0001$) for intermediate-age ($\simeq 1\text{--}2$ Gyr) stars, while a slightly larger metallicity $Z = 0.0004 - 0.001$ is possible for the young (< 1 Gyr) population in the galaxy.

The RR Lyrae candidates, together with the well developed horizontal branch, trace the existence of an important old population in Phoenix. The different spatial distributions of AC, s-pCC, and RR Lyrae variables is consistent with the stellar population gradients found in Phoenix (MGA99), in the sense that the younger populations are progressively more concentrated toward the central part of the galaxy. The gradient in the mean age of the youngest populations in the center of Phoenix, which seems to indicate a propagation of the recent star formation as suggested by MGA99, is also reflected in the spatial distribution of the s-pCC.

We want to thank M. Wischnjewsky⁶ & O. Pevunova for their help in the data reduction, and G. Bono for useful discussions. C.G. wants to thank J.M. Gómez-Forrellad, A.K. Vivas and P. Rodríguez-Gil for obtaining periods of some variables stars at early stages of this work, while she was developing her own code, and G. Bono for useful discussions. C.G. acknowledges partial support from the Spanish Ministry of Science and Technology (Plan Nacional de Investigación Científica, Desarrollo e Investigación Tecnológica, AYA2002-01939), and from the European Structural Funds.

REFERENCES

- Bauer, F. et al. (the EROS collaboration). 1999, *A&A*, 348, 175
- Bertelli, G., Bressan, A., Chiosi, C., Fagotto, F. & Nasi, E. 1994, *A&AS*, 106, 275
- Bono, G. 2003, *Lect. Notes Phys.* 635, 85
- Bono, G., Caputo, F., Santolamazza, P. Cassisi, S. & Piersimoni, A. 1997, *AJ*, 113, 2209
- Clementini, G., Held, E.V., Baldacci, L. & Rizzi, L. 2003, *ApJ*, 588, L85
- Demarque, P. & Hirshfeld, A.W. 1975, *ApJ*, 202, 346
- Dolphin, A.E., Saha, A., Skillman, E.D., Tolstoy, E., Cole, A.A., Dohm-Palmer, R.C., Gallagher, J.S., Mateo, M. & Hoessel, J.G. 2001, *ApJ*, 550, 554
- Dolphin, A.E., Saha, A., Claver, J., Skillman, E.D., Cole, A.A., Gallagher, J.S., Tolstoy, E., Dohm-Palmer, R.C. & Mateo, M. 2002, *AJ*, 123, 3154

⁶Deceased 2002 September

- Dolphin, A.E., Saha, A., Skillman, E.D., Dohm-Palmer, R.C., Tolstoy, E., Cole, A.A., Gallagher, J.S., Hoessel, J.G. & Mateo, M. 2003, AJ, 125, 1261
- Gallart, C. et al. 1999, ApJ, 514, 665
- Gallart, C., Martínez-Delgado, D., Gómez-Flechoso, M.A. & Mateo, M. 2001, AJ, 121, 2572
- Held, E.V., Saviane, I. & Momany, Y. 1999, A&A, 345, 747
- Hirshfeld, A.W. 1980, ApJ, 241, 111
- Landolt, A.U. 1992, AJ, 104, 340
- Layden, A.C. 1998, AJ, 115, 193
- Layden, A.C. & Sarajedini, A. 2000, AJ, 119, 1760
- Martínez-Delgado, D., Gallart, C. & Aparicio, A. 1999 AJ, 118, 862
- Mateo M. 1998, ARA&A 36, 435
- Mateo, M., Fischer, P. & Krzeminski, W. 1995, AJ, 110, 2166
- Nemec, J.M., Nemec, A.F.L. & Lutz, T.E. 1994, AJ, 108, 222
- Norris, J. & Zinn, R. 1975, ApJ, 202, 335
- Pritzl, B.J., Armandroff, T.E., Jacoby, G.H. & Da Costa, G.S. 2002, AJ, 124, 1464
- Pritzl, B.J., Armandroff, T.E., Jacoby, G.H. & Da Costa, G.S. 2003, AJ, 127, 318
- Saha, A. & Hoessel, J.G. 1990. AJ, 99, 97
- Smith, H.A., Silbermann, N.A., Baird, S.R. & Graham, J.A. 1992, AJ, 104, 1430
- Stellingwerf, R.F. 1978, ApJ, 224, 953
- Stetson, P.B. 1987, PASP, 99, 191
- Stetson, P.B. 1990, PASP, 102, 932
- Stetson, P.B. 1994, PASP, 106, 250
- St-Germain, J., Carignan, C., Côté, S. & Oosterloo, T. 1999, AJ, 118, 1235
- Udalski, A., Soszynski, I., Szymanski, M., Kubiak, M., Pietrzynski, G., Wozniak, P. & Zebrun, K. 1999, AcA, 49, 437.

van de Rydt, F., Demers, S. & Kunkel, W.E. 1991, AJ, 102, 130

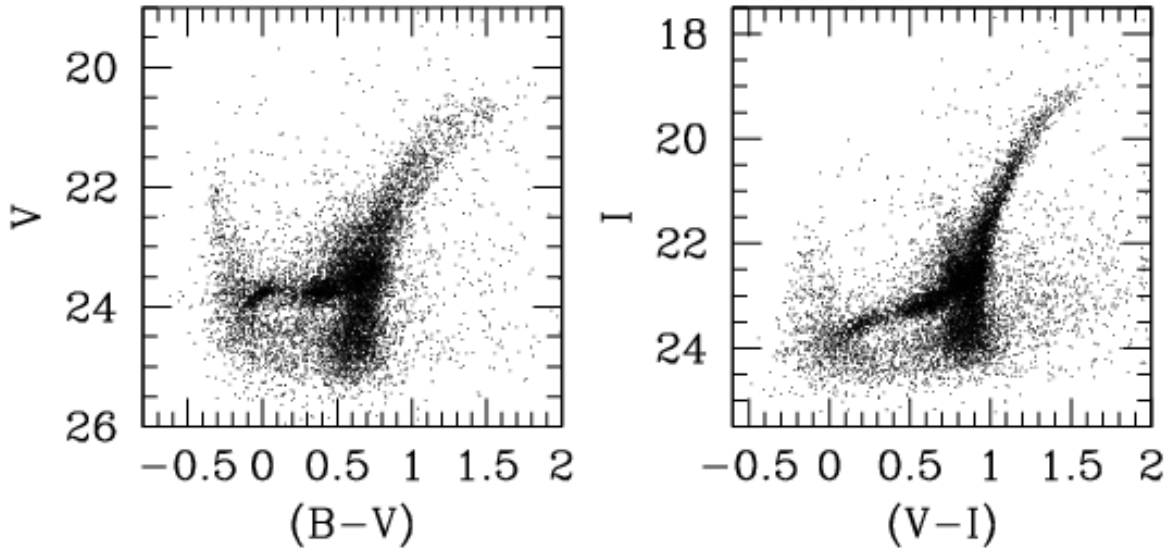


Fig. 1.— $[(B-V), V]$ and $[(V-I), I]$ CMDs of Phoenix.

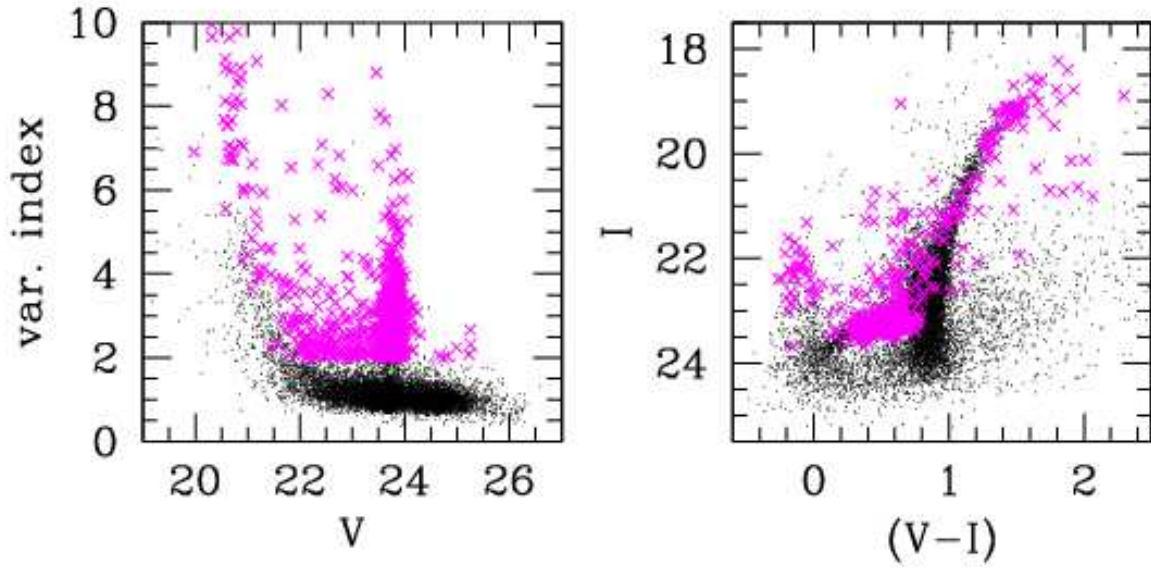


Fig. 2.— Left: First-pass candidate variable stars (crosses). Right: $[(V-I), I]$ CMD of Phoenix, with the first-pass candidate variable stars highlighted. A substantial number of spurious detections appear in this sample.

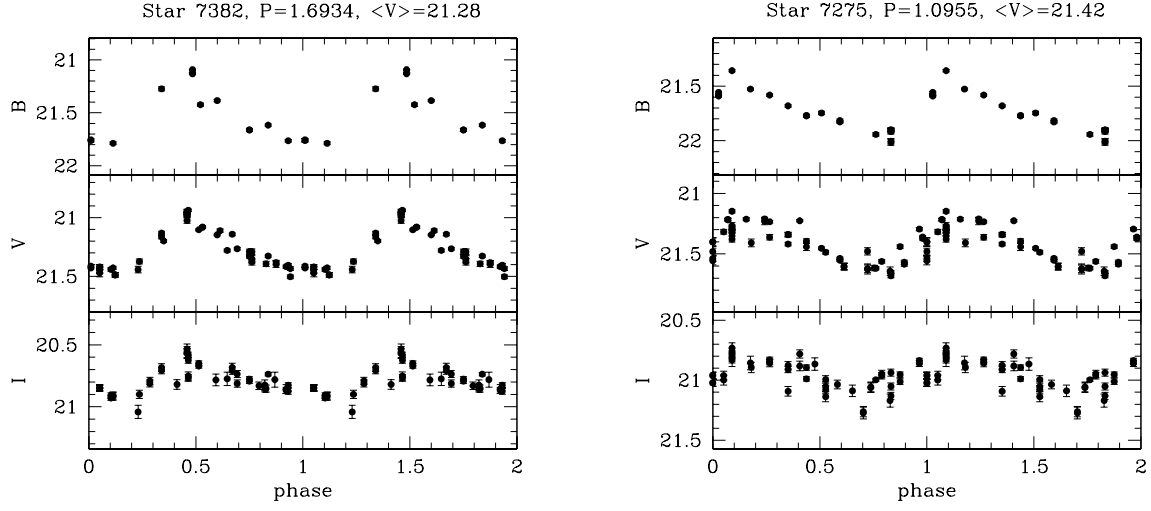


Fig. 3.— a) B , V and I light curves for the Phoenix Cepheids. Data are repeated over a second cycle for clarity.

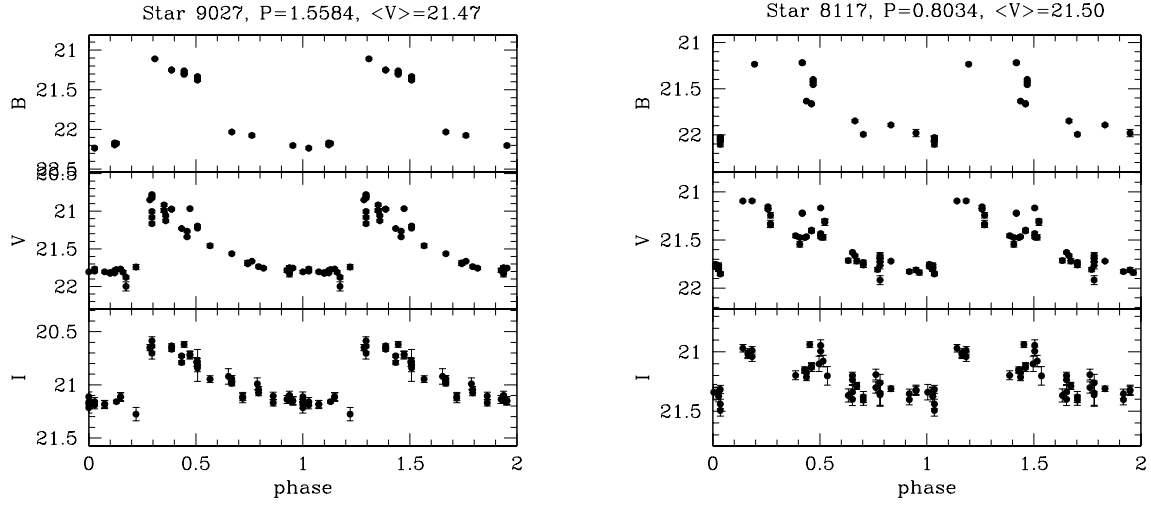


Fig. 3.— b)

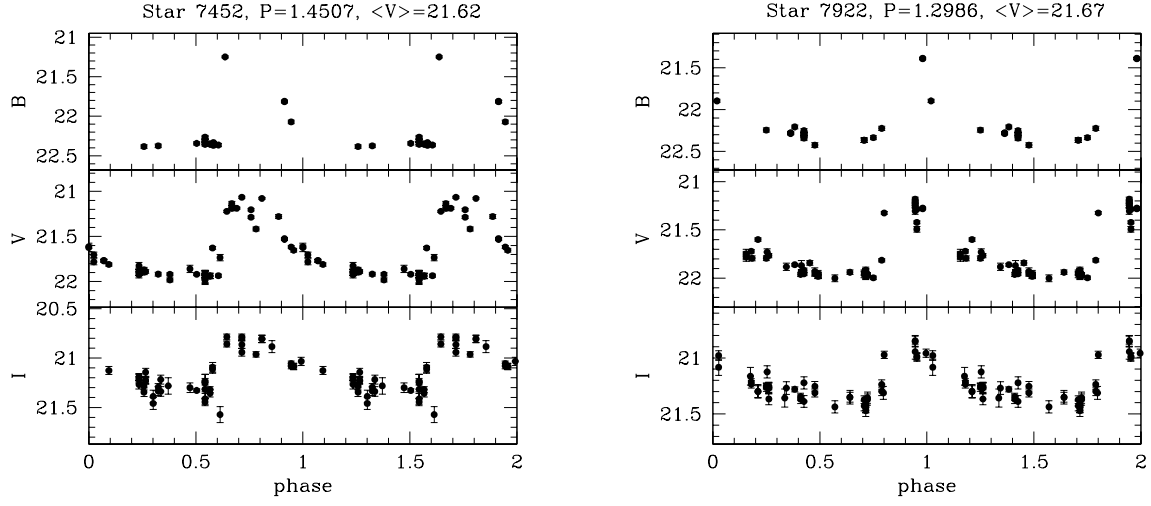


Fig. 3.— c)

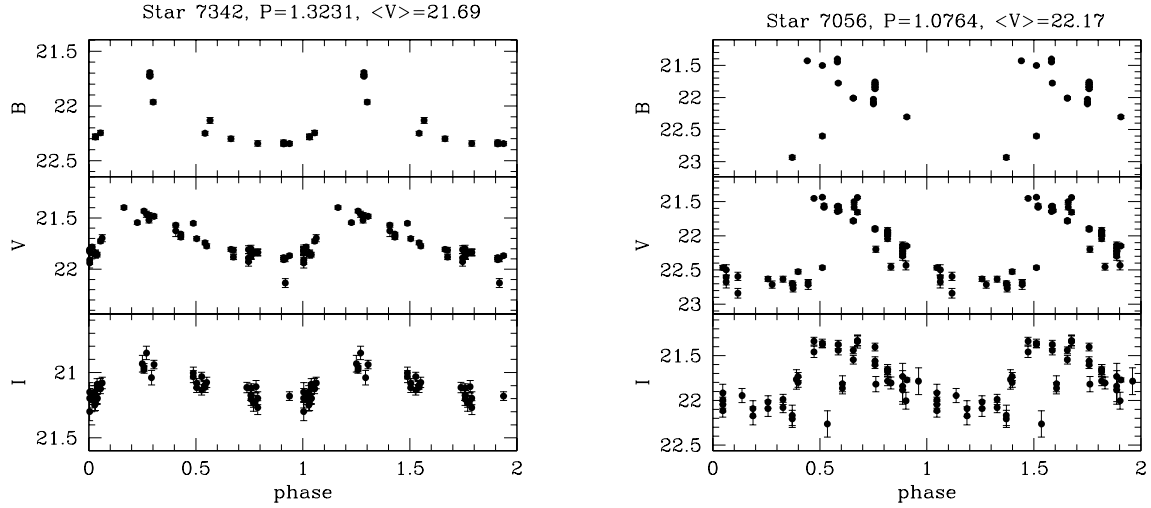


Fig. 3.— d)

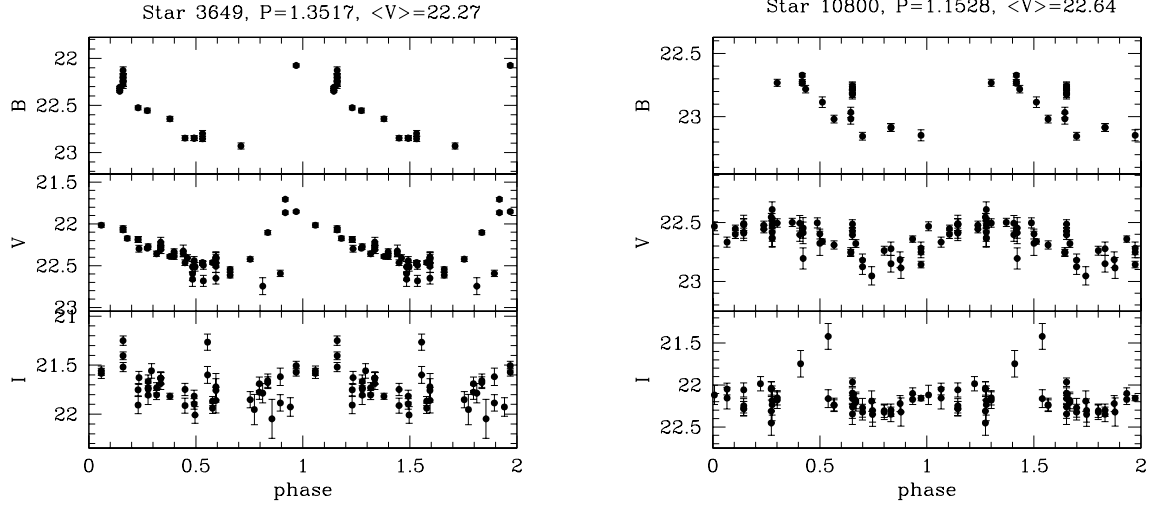


Fig. 3.— e)

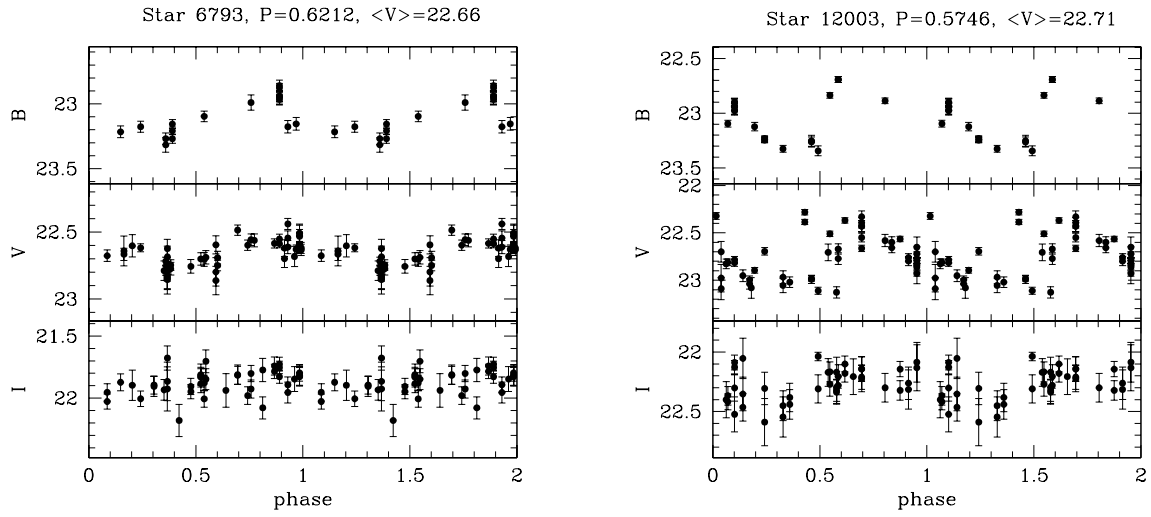


Fig. 3.— f)

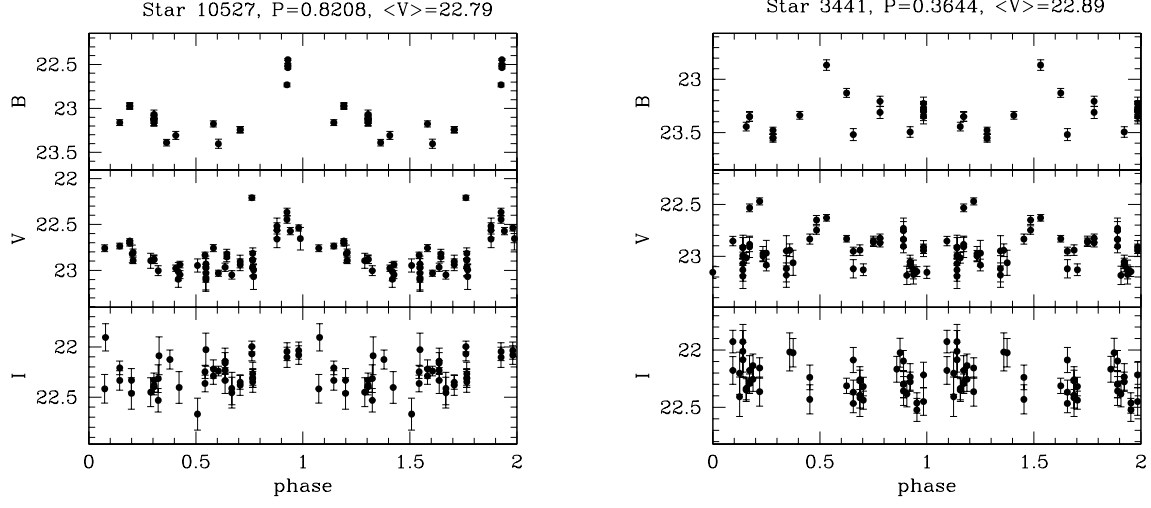


Fig. 3.— g)

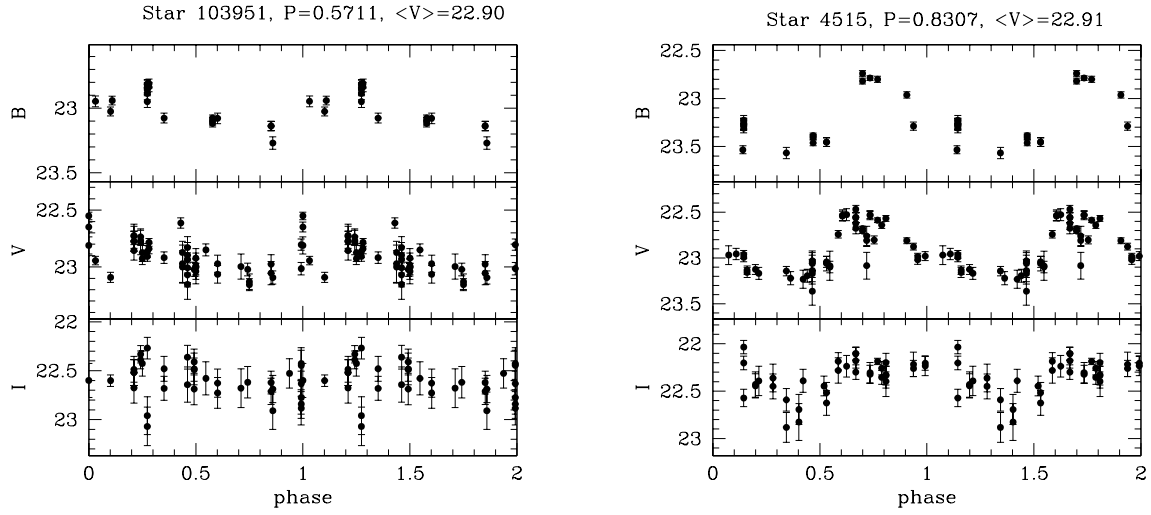


Fig. 3.— h)

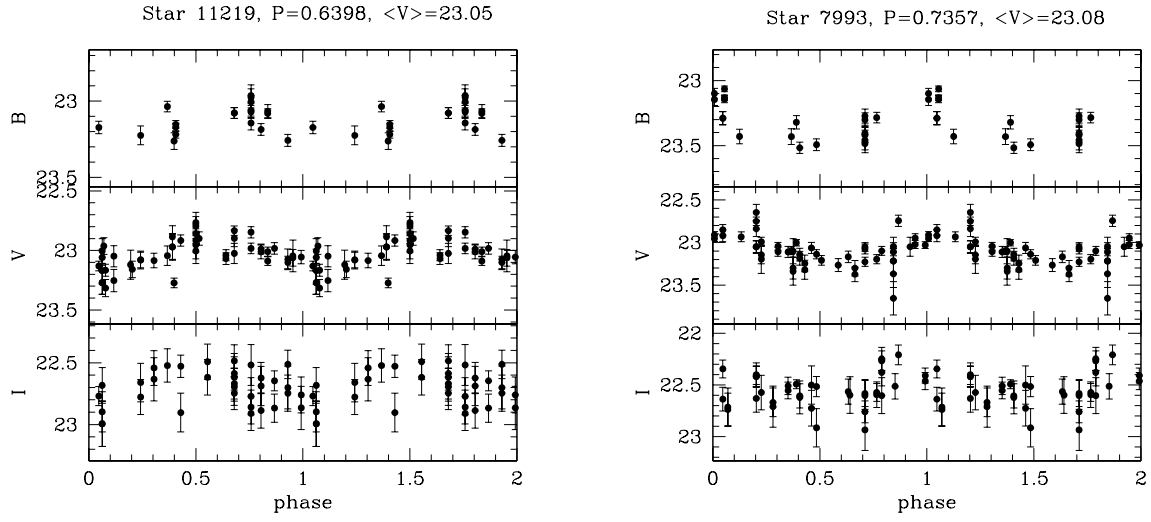


Fig. 3.— i)

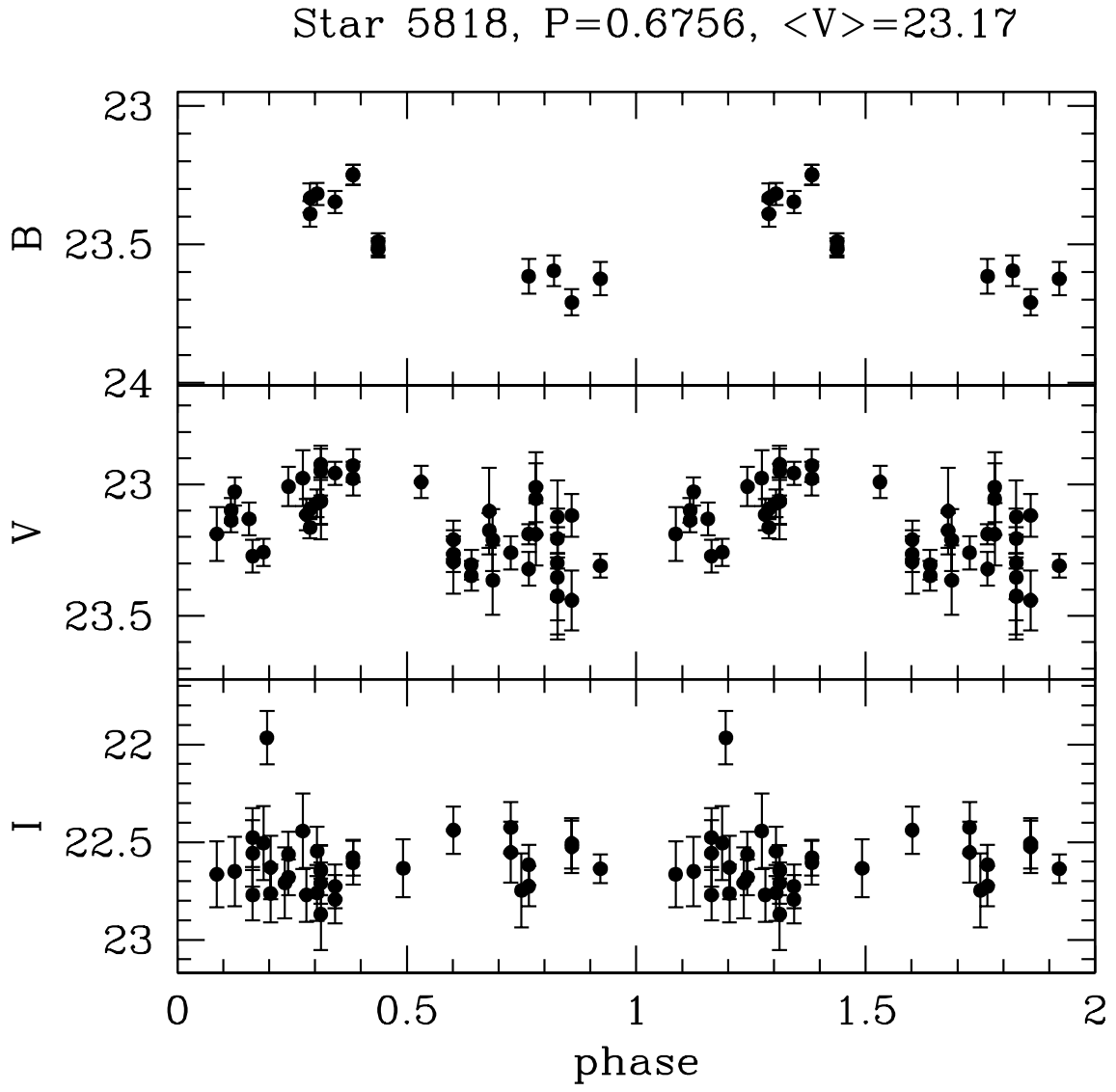


Fig. 3.— j)

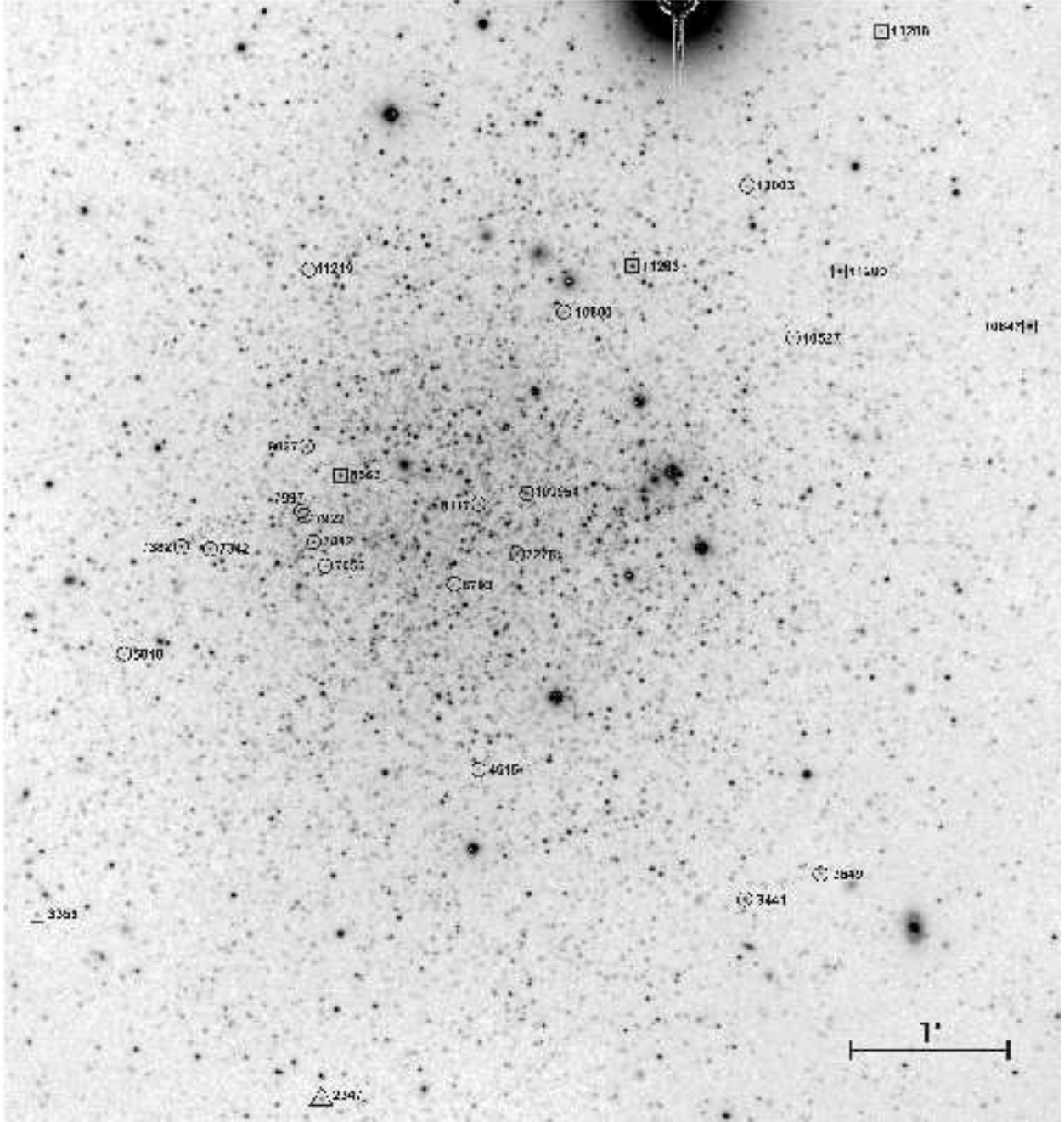


Fig. 4.— Finder chart for the Phoenix variable stars. Confirmed Cepheid variables are marked with circles, candidate long-period variables with squares, and the candidate eclipsing binary with a triangle. North is down and east is to the left.

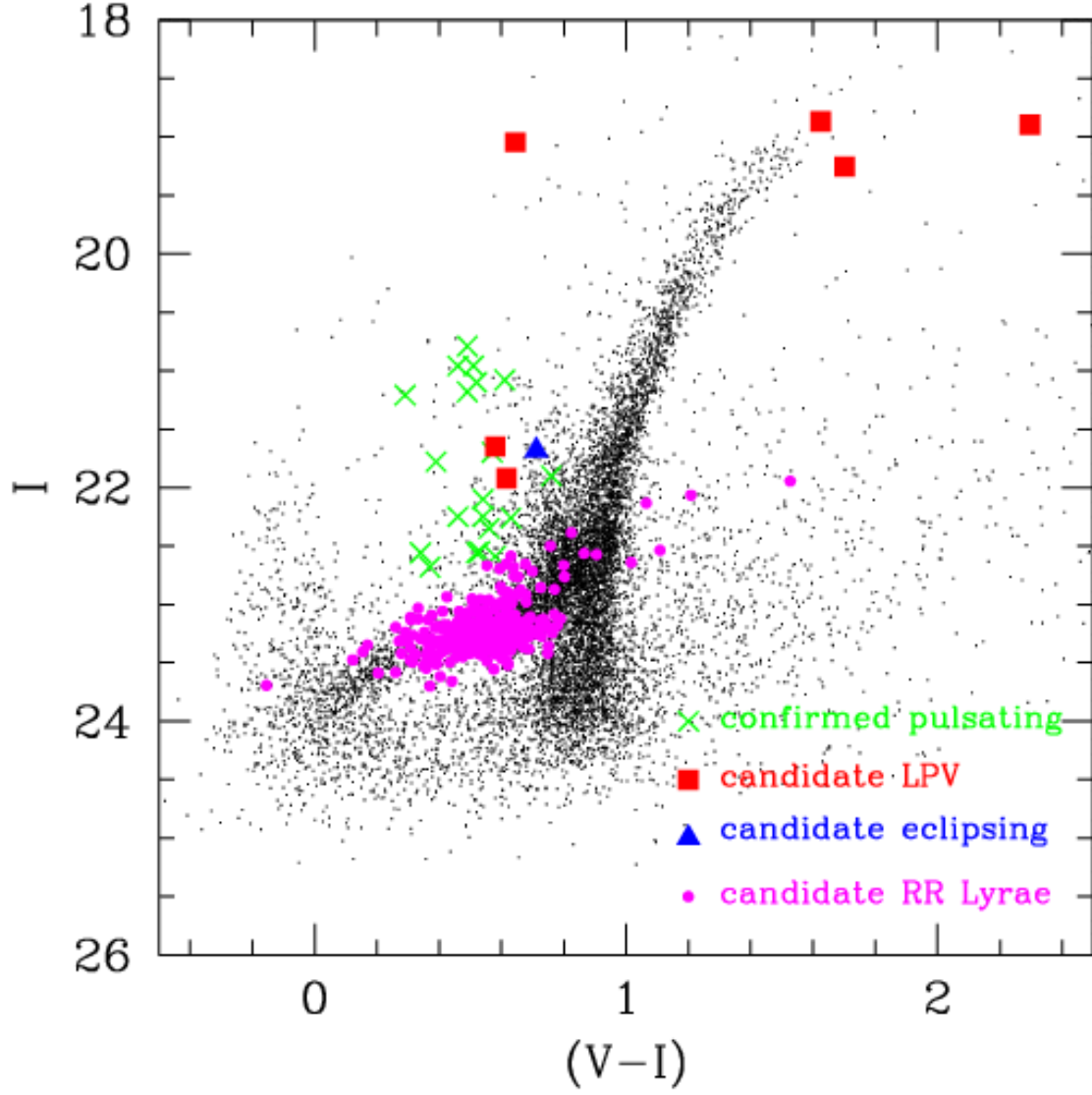


Fig. 5.— Confirmed pulsating (crosses) and long-period (squares) variables, and the candidate eclipsing binary star (triangle). The 396 candidate RR Lyrae stars are shown as small circles.

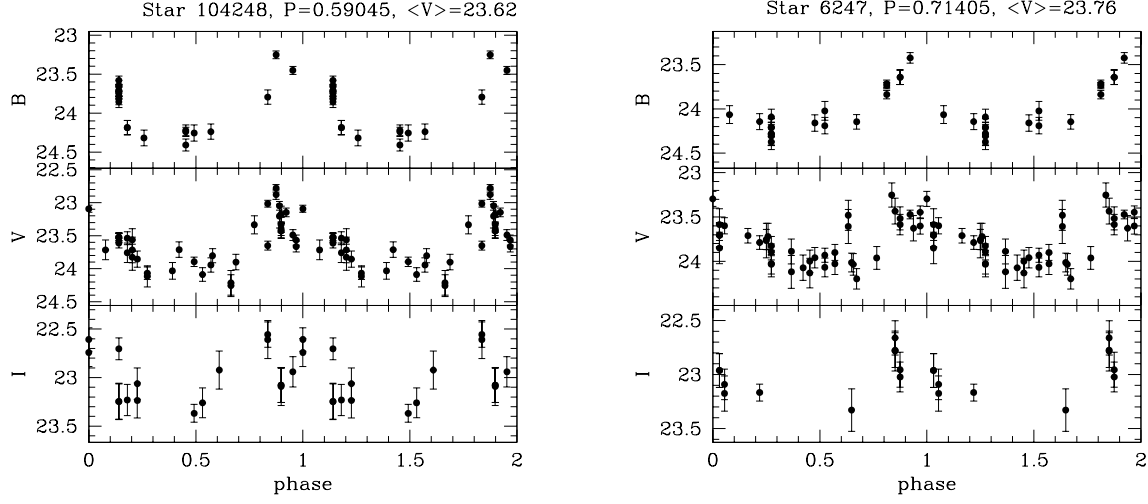


Fig. 6.— a) B , V and I light curves for a sample of Phoenix confirmed RR Lyrae. Not all the RR Lyrae candidates have been analyzed for periods. Data are repeated over a second cycle for clarity.

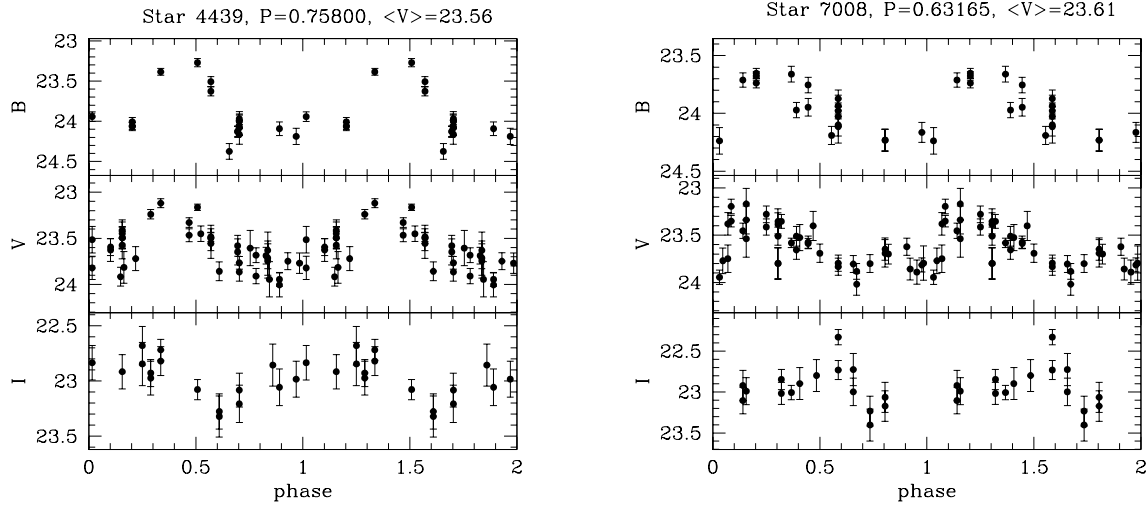


Fig. 6.— b)

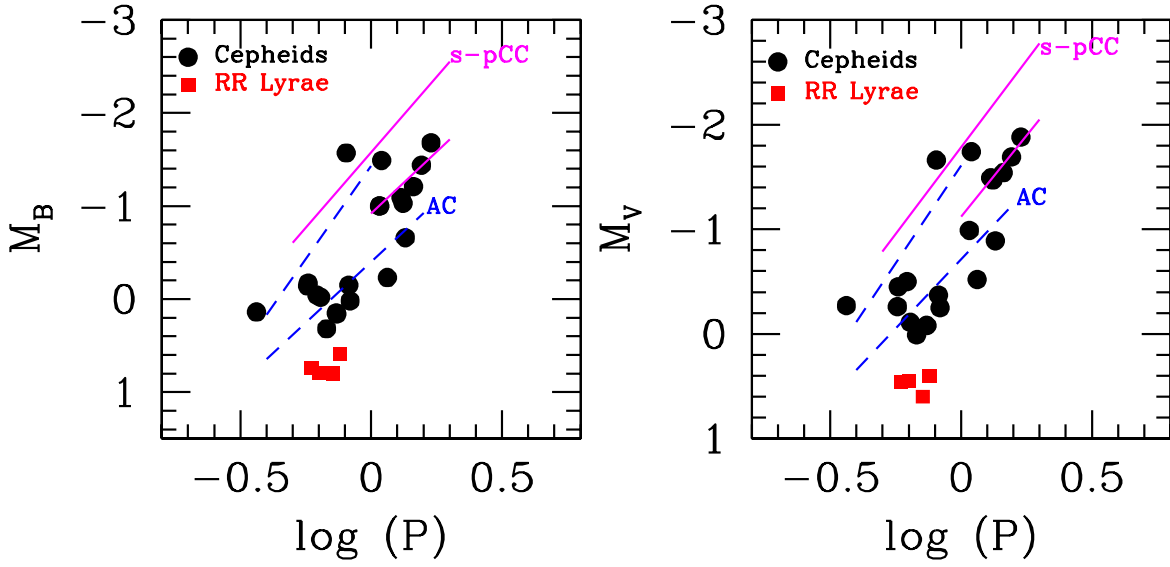


Fig. 7.— Period-luminosity (PL) diagrams (in the B and V bands) for the Phoenix Cepheids. The PL relations obtained for dSph AC by Pritzl et al. (2002) are represented as dashed lines, and the PL relations for ($P \leq 2$ days) OGLE SMC s-pCC as solid lines (see text for details). The four RR Lyrae variables for which periods have been obtained are included in the plot.

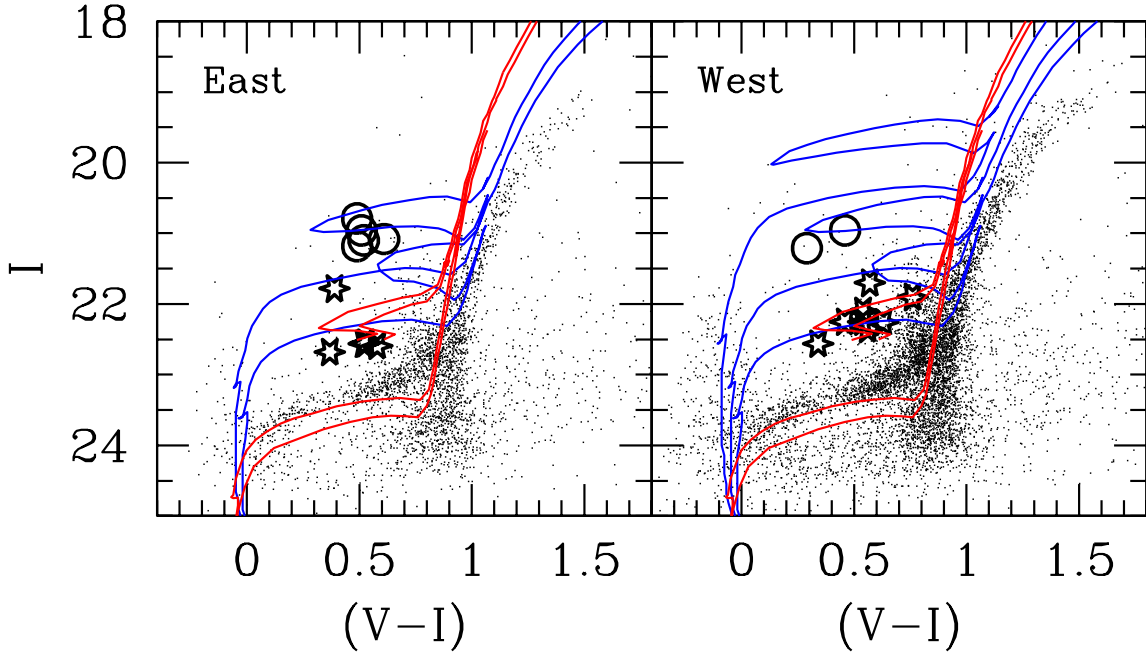


Fig. 8.— CMDs of the eastern and western parts of Phoenix. The east/west division has been made in order to keep separate the stars belonging to the young association located in the west part. It does not divide the galaxy exactly in half, and thus the sequences appear more populated in the west CMD. The ratio of main sequence *plus* blue-loop stars ($-0.5 \leq (V - I) \leq 0.1$), $21 \leq I \leq 23.5$) to stars near the tip of the RGB ($(V - I) \leq 1.0$, $I \leq 20$) is however significantly larger in the west part (1.1 ± 0.2 vs 0.4 ± 0.2), where the blue stars also extend to brighter magnitudes, indicating younger ages. s-pCC and AC are represented as circles and stars respectively. Isochrones from Bertelli et al. (1994) for $Z = 0.001$ and ages 200, 400 and 600 Myr, and for $Z = 0.0001$ and 1.3 and 1.6 Gyr have been superimposed. Note how the position of the s-pCC are well fit by the younger isochrones, while the AC are best fit by the isochrones older than 1 Gyr.

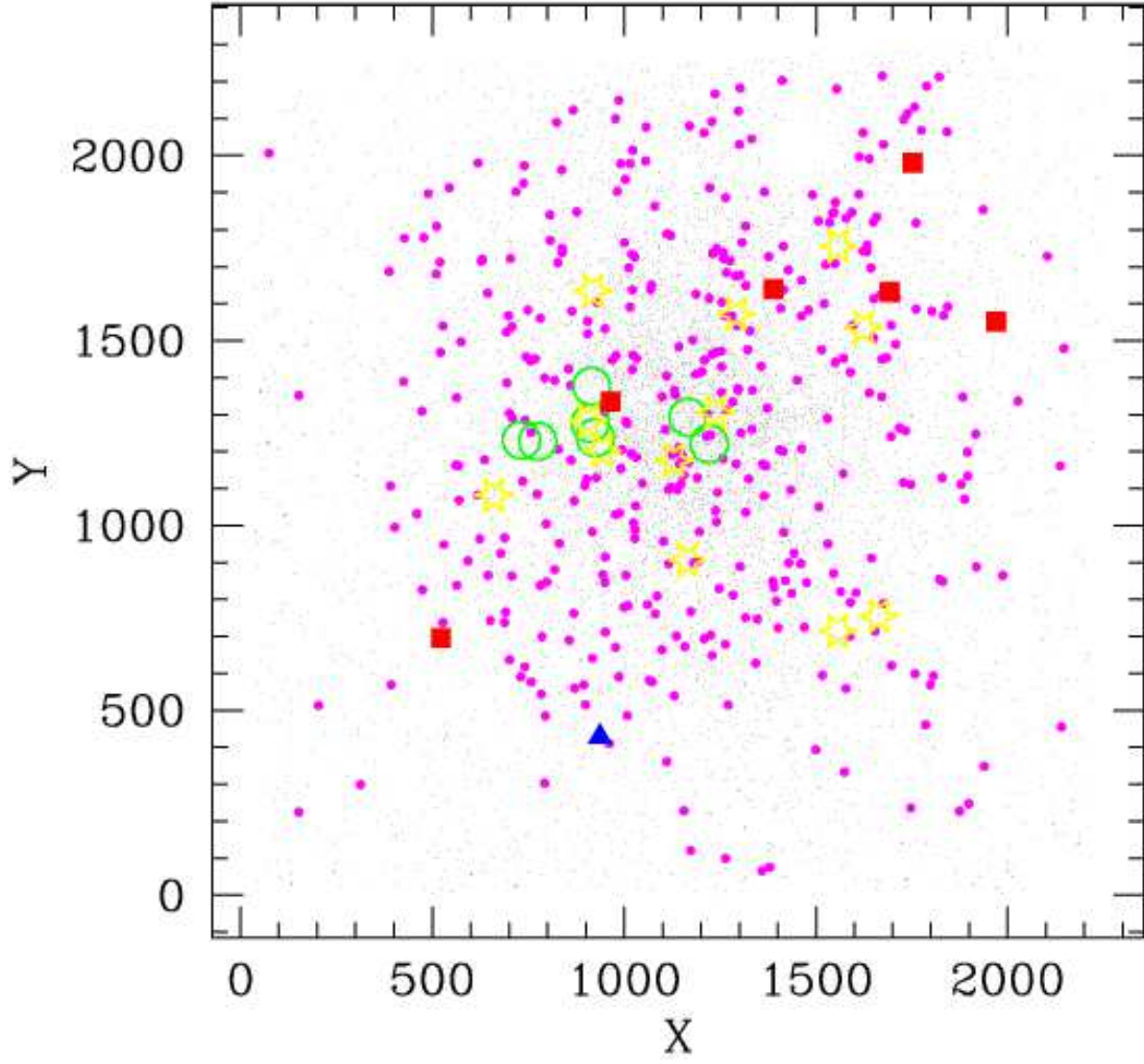


Fig. 9.— Spatial distribution of the s-pCC (circles), AC (stars) long period (squares), and the candidate eclipsing binary star (triangle). The 396 candidate RR Lyrae stars are shown as small circles.

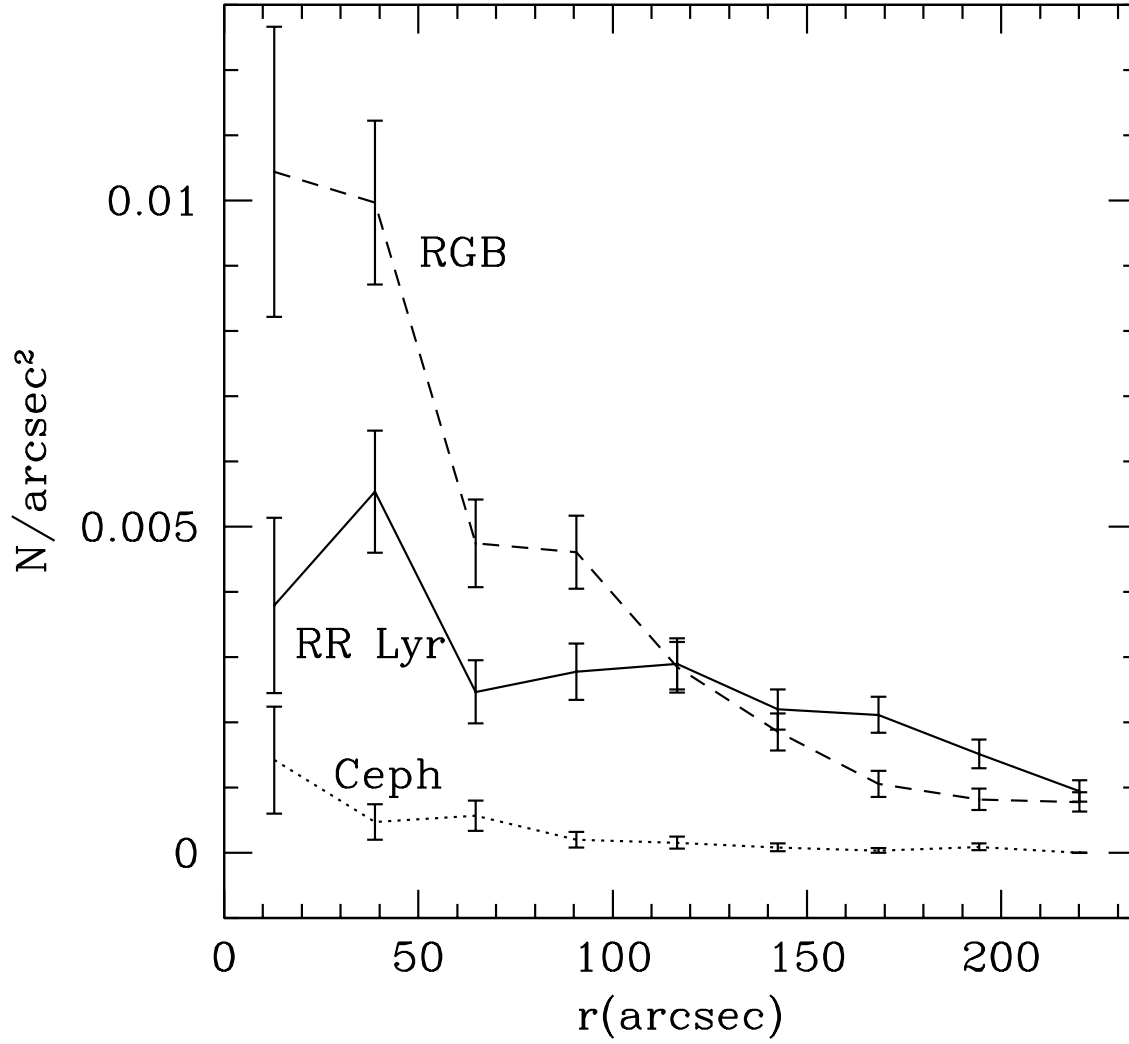


Fig. 10.— Radial counts of RGB stars ($I \leq 20.5$, dashed line), RR Lyrae variable star candidates and Cepheid variables.

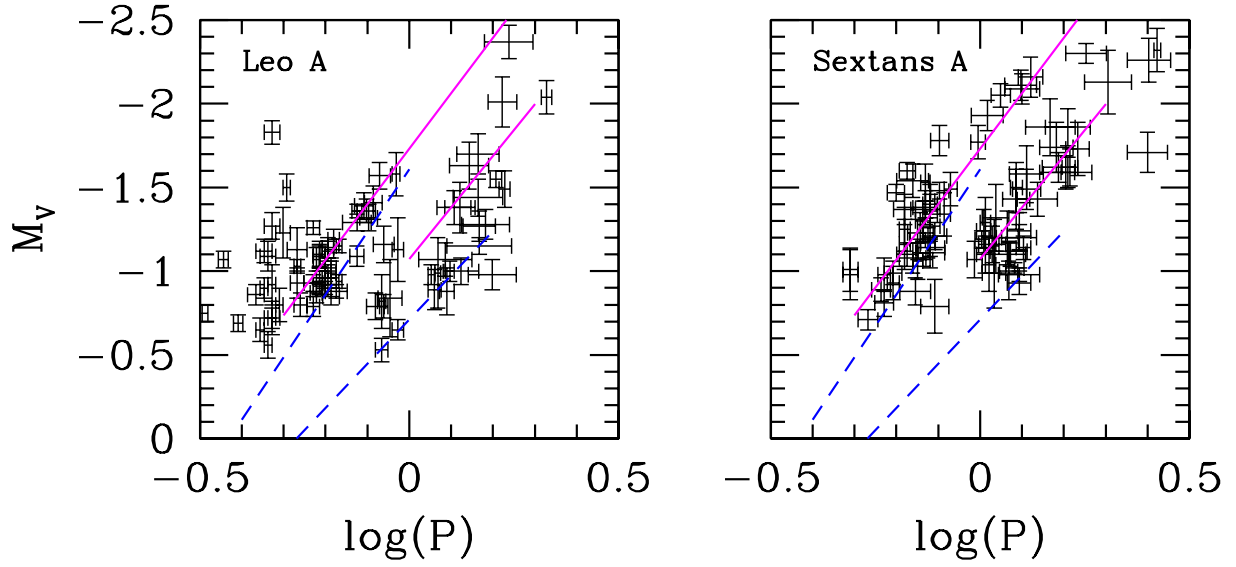


Fig. 11.— Period-luminosity (PL) diagrams for the Leo A (left) and Sextans A (right) Cepheids. Distance modulus $(m-M)_V = 24.54$ and 25.72 , according to Dolphin et al. (2002) and Dolphin et al. (2003) respectively, have been assumed. The PL relations obtained for dSph AC and OGLE SMC s-pCC are represented as in Figure 7.

Table 1. Observation Log

| Image ID | JD –2400000.0 | T _{exp} (sec) | Filter | seeing |
|--|---------------|------------------------|----------|--------|
| <i>ESO Archival data: 3.6m NTT w/EMMI, December 23, 1992</i> | | | | |
| emmi1992v1.imh | 48979.652773 | 720.000 | <i>V</i> | 0.8 |
| emmi1992v2.imh | 48979.663096 | 720.000 | <i>V</i> | 0.9 |
| emmi1992v3.imh | 48979.684380 | 720.000 | <i>V</i> | 0.9 |
| LCO 100", February 8-16, 1997 | | | | |
| clco2031 | 50489.537980 | 300.070 | <i>V</i> | 1.1 |
| clco2032 | 50489.545827 | 300.050 | <i>V</i> | 1.0 |
| clco2033 | 50489.550514 | 300.060 | <i>V</i> | 0.9 |
| clco2037 | 50489.569090 | 300.050 | <i>V</i> | 1.0 |
| clco2038 | 50489.573673 | 300.070 | <i>V</i> | 1.1 |
| clco2039 | 50489.578164 | 300.070 | <i>V</i> | 1.2 |
| clco3036 | 50490.529709 | 300.060 | <i>V</i> | 1.1 |
| clco3037 | 50490.534142 | 300.060 | <i>V</i> | 1.1 |
| clco3038 | 50490.538575 | 300.040 | <i>V</i> | 0.9 |
| clco3043 | 50490.573770 | 600.050 | <i>V</i> | 1.1 |
| clco5025 | 50492.584464 | 600.040 | <i>V</i> | 1.1 |
| clco6029 | 50493.545780 | 600.050 | <i>V</i> | 1.4 |
| clco6030 | 50493.553685 | 600.070 | <i>V</i> | 1.4 |
| clco7025 | 50494.532872 | 600.050 | <i>V</i> | 1.6 |
| clco8029 | 50495.563285 | 600.040 | <i>V</i> | 1.9 |
| clco9028 | 50496.579857 | 600.040 | <i>V</i> | 1.6 |
| clco1027 | 50488.564815 | 300.050 | <i>I</i> | 0.9 |
| clco2034 | 50489.555583 | 300.050 | <i>I</i> | 0.8 |
| clco2035 | 50489.560016 | 300.050 | <i>I</i> | 0.9 |
| clco2036 | 50489.564449 | 300.060 | <i>I</i> | 0.8 |
| clco3040 | 50490.549651 | 600.050 | <i>I</i> | 1.0 |
| clco3041 | 50490.557555 | 600.050 | <i>I</i> | 1.0 |

Table 1—Continued

| Image ID | JD –2400000.0 | T _{exp} (sec) | Filter | seeing |
|--|---------------|------------------------|----------|--------|
| clco3042 | 50490.565472 | 600.050 | <i>I</i> | 0.9 |
| clco5024 | 50492.576397 | 600.050 | <i>I</i> | 1.2 |
| clco6027 | 50493.528779 | 600.060 | <i>I</i> | 1.2 |
| clco6028 | 50493.537598 | 600.060 | <i>I</i> | 1.0 |
| clco7024 | 50494.524724 | 600.060 | <i>I</i> | 1.3 |
| clco8030 | 50495.571467 | 600.050 | <i>I</i> | 1.6 |
| clco9027 | 50496.571801 | 600.060 | <i>I</i> | 1.2 |
| LCO 100”, TEK5, November 22-26, 1997 | | | | |
| blco2019 | 50774.518148 | 900.060 | <i>V</i> | 1.3 |
| blco2020 | 50774.529768 | 900.070 | <i>V</i> | 0.9 |
| blco3025 | 50775.639881 | 900.040 | <i>V</i> | 1.0 |
| blco3026 | 50775.651374 | 900.070 | <i>V</i> | 0.9 |
| blco4010 | 50776.640602 | 900.040 | <i>V</i> | 0.7 |
| blco4011 | 50776.652117 | 900.060 | <i>V</i> | 0.8 |
| blco5041 | 50777.603592 | 900.040 | <i>V</i> | 0.8 |
| blco5042 | 50777.615177 | 900.060 | <i>V</i> | 0.8 |
| blco6051 | 50778.574973 | 900.060 | <i>V</i> | 1.3 |
| blco6052 | 50778.586477 | 900.070 | <i>V</i> | 1.1 |
| <i>ESO Archival data:</i> 3.6m NTT w/SUSI2, July 16, 1998 | | | | |
| susijul98v | 51011.931727 | 1800.000 | <i>V</i> | 1.3 |
| susijul98i | 51011.947320 | 801.193 | <i>I</i> | 1.3 |
| <i>ESO Archival data:</i> 3.6m NTT w/SUSI2, October 28, 1998 | | | | |
| susinov98b1 | 51114.759908 | 399.999 | <i>B</i> | 0.8 |
| susinov98b2 | 51114.765005 | 400.000 | <i>B</i> | 0.7 |
| susinov98b3 | 51114.770044 | 399.999 | <i>B</i> | 0.7 |

Table 1—Continued

| Image ID | JD –2400000.0 | T _{exp} (sec) | Filter | seeing |
|---|------------------|------------------------|----------|--------|
| susinov98b4 | 51114.775088 | 400.000 | <i>B</i> | 0.7 |
| susinov98b5 | 51114.780112 | 399.999 | <i>B</i> | 0.9 |
| susinov98b6 | 51114.785211 | 400.000 | <i>B</i> | 0.7 |
| susinov98v1 | 51114.789725 | 300.000 | <i>V</i> | 0.9 |
| susinov98v2 | 51114.793617 | 299.999 | <i>V</i> | 0.7 |
| susinov98i1 | 51114.799479 | 399.999 | <i>I</i> | 0.7 |
| susinov98i2 | 51114.804636 | 399.999 | <i>I</i> | 0.7 |
| susinov98i3 | 51114.809681 | 399.999 | <i>I</i> | 0.7 |
| LCO 100”, TEK5, September 11-14, 1998 | | | | |
| dlco381 | 2451070.85641682 | 900.050 | <i>B</i> | 1.5 |
| dlco382 | 2451070.87038687 | 900.060 | <i>B</i> | 1.5 |
| <i>ESO Archival data: VLT-Antu w/FORS1, August 20, 1999</i> | | | | |
| fors1999b1 | 51410.814718 | 599.976 | <i>B</i> | 0.8 |
| fors1999b2 | 51410.822354 | 600.000 | <i>B</i> | 0.9 |
| fors1999b3 | 51410.829979 | 600.000 | <i>B</i> | 0.9 |
| fors1999r1 | 51410.836018 | 299.989 | R | 0.8 |
| fors1999r2 | 51410.840160 | 300.000 | R | 0.9 |
| VLT-Antu w/FORS1, September 15, 1999 | | | | |
| phob | 51436.731704 | 300.000 | <i>B</i> | 1.0 |
| phoi | 51436.898504 | 300.000 | <i>I</i> | 0.8 |
| phor | 51436.739953 | 299.998 | R | 0.9 |
| phov | 51436.735826 | 300.000 | <i>V</i> | 0.6 |
| <i>ESO Archival data: VLT-Antu w/FORS1, July 7-8, 2000</i> | | | | |

Table 1—Continued

| Image ID | JD –2400000.0 | T _{exp} (sec) | Filter | seeing |
|--------------------------------------|---------------|------------------------|----------|--------|
| fors2000b1 | 51550.540040 | 299.993 | <i>B</i> | 0.8 |
| fors2000b2 | 51550.544182 | 299.992 | <i>B</i> | 0.7 |
| fors2000b3 | 51551.567297 | 299.986 | <i>B</i> | 0.7 |
| fors2000v1 | 51550.529901 | 399.982 | <i>V</i> | 0.8 |
| fors2000v2 | 51550.535205 | 399.983 | <i>V</i> | 0.8 |
| fors2000v3 | 51551.562306 | 399.972 | <i>V</i> | 0.8 |
| LCO 100”, TEK5, November 25-29, 2000 | | | | |
| b2ccd2038 | 51873.612653 | 1200.030 | <i>B</i> | 0.9 |
| b2ccd3041 | 51874.630813 | 1200.030 | <i>B</i> | 0.8 |
| b2ccd4040 | 51875.644344 | 1200.030 | <i>B</i> | 0.8 |
| b2ccd5042 | 51876.688254 | 1200.040 | <i>B</i> | 0.9 |
| b2ccd6037 | 51877.621985 | 1200.030 | <i>B</i> | 0.8 |
| b2ccd2034 | 51873.579240 | 450.040 | <i>V</i> | 0.8 |
| b2ccd2035 | 51873.585722 | 450.040 | <i>V</i> | 0.8 |
| b2ccd3037 | 51874.597146 | 450.040 | <i>V</i> | 0.8 |
| b2ccd3038 | 51874.603384 | 450.040 | <i>V</i> | 0.8 |
| b2ccd4037 | 51875.614959 | 900.030 | <i>V</i> | 0.8 |
| b2ccd5043 | 51876.701564 | 900.030 | <i>V</i> | 0.8 |
| b2ccd6038 | 51877.635306 | 900.030 | <i>V</i> | 0.9 |
| b2ccd2036f | 51873.593001 | 600.030 | <i>I</i> | 0.7 |
| b2ccd2037f | 51873.601068 | 600.040 | <i>I</i> | 0.7 |
| b2ccd3039f | 51874.611278 | 600.030 | <i>I</i> | 0.7 |
| b2ccd3040f | 51874.619240 | 600.040 | <i>I</i> | 0.7 |
| b2ccd4038f | 51875.624854 | 600.030 | <i>I</i> | 0.7 |
| b2ccd4039f | 51875.632817 | 600.050 | <i>I</i> | 0.7 |
| b2ccd5044f | 51876.711366 | 600.030 | <i>I</i> | 1.0 |
| b2ccd5045f | 51876.719283 | 600.040 | <i>I</i> | 0.8 |
| b2ccd6039f | 51877.645086 | 600.030 | <i>I</i> | 0.8 |
| b2ccd6040f | 51877.653037 | 600.040 | <i>I</i> | 0.9 |

Table 1—Continued

| Image ID | JD –2400000.0 | T _{exp} (sec) | Filter | seeing |
|--------------------------------------|---------------|------------------------|----------|--------|
| LCO 100”, TEK5, December 13-21, 2001 | | | | |
| fccd1063 | 52256.648676 | 1200.040 | <i>V</i> | 1.1 |
| fccd2051 | 52257.637329 | 1200.030 | <i>V</i> | 0.8 |
| fccd3047 | 52258.643909 | 1200.040 | <i>V</i> | 1.0 |
| fccd4048 | 52259.614716 | 1200.040 | <i>V</i> | 1.0 |
| fccd5060 | 52260.647428 | 1200.050 | <i>V</i> | 1.7 |
| fccd6052 | 52261.662607 | 1200.030 | <i>V</i> | 1.0 |
| fccd6053 | 52261.680418 | 1200.040 | <i>V</i> | 1.3 |
| fccd7038 | 52262.556439 | 1200.030 | <i>V</i> | 0.9 |
| fccd7049 | 52262.710307 | 1200.030 | <i>V</i> | 1.2 |
| fccd9056 | 52264.678295 | 1200.030 | <i>V</i> | 0.9 |
| fccd10058 | 52265.655478 | 1200.030 | <i>V</i> | 1.2 |
| fccd11053 | 52266.649246 | 1200.030 | <i>V</i> | 1.0 |
| fccd1064 | 52256.664253 | 900.030 | <i>I</i> | 0.9 |
| fccd1065 | 52256.677401 | 900.030 | <i>I</i> | 1.1 |
| fccd2052 | 52257.651575 | 900.030 | <i>I</i> | 0.8 |
| fccd2053 | 52257.663323 | 900.040 | <i>I</i> | 0.7 |
| fccd3045 | 52258.618239 | 900.040 | <i>I</i> | 0.8 |
| fccd3046 | 52258.629755 | 900.030 | <i>I</i> | 0.7 |
| fccd4049 | 52259.628071 | 900.030 | <i>I</i> | 0.9 |
| fccd4050 | 52259.639599 | 900.040 | <i>I</i> | 0.8 |
| fccd5061 | 52260.662381 | 900.030 | <i>I</i> | 1.2 |
| fccd5062 | 52260.675436 | 900.040 | <i>I</i> | 1.3 |
| fccd6054 | 52261.694225 | 900.030 | <i>I</i> | 1.5 |
| fccd6055 | 52261.705672 | 900.050 | <i>I</i> | 1.4 |
| fccd7039 | 52262.569945 | 900.030 | <i>I</i> | 0.7 |
| fccd7040 | 52262.581727 | 900.040 | <i>I</i> | 0.8 |
| fccd7047 | 52262.684973 | 900.040 | <i>I</i> | 1.2 |
| fccd7048 | 52262.696615 | 900.040 | <i>I</i> | 1.2 |

Table 1—Continued

| Image ID | JD –2400000.0 | T _{exp} (sec) | Filter | seeing |
|-----------|---------------|------------------------|----------|--------|
| fccd9057 | 52264.691743 | 900.030 | <i>I</i> | 0.9 |
| fccd9058 | 52264.703143 | 900.030 | <i>I</i> | 0.8 |
| fccd10059 | 52265.669088 | 900.030 | <i>I</i> | 1.1 |
| fccd10060 | 52265.680442 | 900.030 | <i>I</i> | 1.5 |
| fccd11054 | 52266.663944 | 900.030 | <i>I</i> | 0.8 |
| fccd11055 | 52266.505285 | 900.030 | <i>I</i> | 0.8 |

Table 2. Confirmed variable stars

| ID ^a | X | Y | Period | mean B | mean V | mean I | Sub-type |
|--------------------------------------|----------|----------|----------------------|----------|----------|----------|--------------------|
| Cepheid (AC or s-pCC) variable stars | | | | | | | |
| 7382 ^c | 732.369 | 1231.179 | 1.69340 | 21.50 | 21.28 | 20.79 | s-pCC |
| 7275 | 1222.072 | 1220.612 | 1.09550 | 21.69 | 21.42 | 20.96 | s-pCC |
| 9027 ^d | 914.971 | 1376.685 | 1.55840 | 21.74 | 21.47 | 20.96 | s-pCC |
| 8117 | 1166.702 | 1292.789 | 0.80340 | 21.61 | 21.50 | 21.21 | s-pCC |
| 7452 | 925.259 | 1237.570 | 1.45070 | 21.97 | 21.62 | 21.10 | s-pCC |
| 7922 ^e | 911.648 | 1276.491 | 1.29860 | 22.09 | 21.67 | 21.18 | s-pCC |
| 7342 | 774.810 | 1227.815 | 1.32315 | 22.15 | 21.69 | 21.08 | s-pCC |
| 7056 ^f | 942.529 | 1202.454 | 1.07640 | 22.18 | 22.17 | 21.78 | s-pCC ^g |
| 3649 | 1664.440 | 755.690 | 1.35170 | 22.52 | 22.27 | 21.70 | AC |
| 10800 | 1292.180 | 1572.292 | 1.15280 ^b | 22.95 | 22.64 | 22.10 | AC |
| 10800 | 1292.180 | 1572.292 | 7.54886 | 22.89 | 22.66 | 22.11 | |
| 6793 | 1129.687 | 1176.729 | 0.62118 ^b | 23.14 | 22.66 | 21.90 | AC |
| 6793 | 1129.687 | 1176.729 | 1.63969 | 23.18 | 22.65 | 21.89 | |
| 12003 | 1557.913 | 1755.501 | 0.57465 | 23.01 | 22.71 | 22.25 | AC |
| 10527 | 1624.325 | 1535.367 | 0.82080 | 23.03 | 22.79 | 22.25 | AC |
| 3441 | 1556.875 | 714.576 | 0.36438 | 23.32 | 22.89 | 22.26 | AC |
| 103951 | 1238.072 | 1306.065 | 0.57113 | 23.04 | 22.90 | 22.56 | AC |
| 4515 | 1165.694 | 907.197 | 0.83070 | 23.20 | 22.91 | 22.35 | AC |
| 11219 | 918.179 | 1633.937 | 0.63985 | 23.16 | 23.05 | 22.68 | AC |
| 7993 | 906.453 | 1282.576 | 0.13553 | 23.37 | 23.09 | 22.53 | |
| 7993 | 906.453 | 1282.576 | 0.73566 ^b | 23.33 | 23.08 | 22.56 | AC |
| 7993 | 906.453 | 1282.576 | 0.73927 ^b | 23.34 | 23.08 | 22.55 | AC |
| 5818 | 660.618 | 1082.305 | 0.67564 ^b | 23.50 | 23.17 | 22.59 | AC |
| 5818 | 660.618 | 1082.305 | 1.97859 | 23.47 | 23.13 | 22.58 | |
| Sample RR Lyrae | | | | | | | |
| 104248 | 1130.850 | 1365.450 | 0.59045 | 23.92 | 23.62 | 22.99 | |

Table 2—Continued

| ID ^a | X | Y | Period | mean B | mean V | mean I | Sub-type |
|---------------------------------|----------|----------|---------|----------|----------|----------|----------|
| 6247 | 1324.488 | 1126.068 | 0.71405 | 23.98 | 23.76 | 23.12 | |
| 4439 | 1116.305 | 896.573 | 0.75800 | 23.77 | 23.56 | 22.97 | |
| 7008 | 1895.248 | 1198.236 | 0.63165 | 23.97 | 23.61 | 22.97 | |
| Candidate Long Period Variables | | | | | | | |
| 10647 | 1969.314 | 1551.632 | | 19.80 | 19.69 | 19.05 | |
| 11200 | 1692.356 | 1631.371 | | 22.21 | 20.49 | 18.87 | |
| 8563 | 964.725 | 1334.615 | | 22.15 | 20.96 | 19.25 | |
| 11263 | 1389.933 | 1638.590 | | 25.57 | 21.19 | 18.90 | |
| 13288 | 1752.993 | 1980.251 | | 21.93 | 22.23 | 21.65 | |
| 3359 | 522.283 | 696.066 | | 23.17 | 22.54 | 21.92 | |
| Candidate eclipsing binary | | | | | | | |
| 2347 | 936.704 | 429.077 | | 22.35 | 22.39 | 21.68 | |

^aStars listed multiple times have more than one possible period producing an acceptable light curve

^bMost likely period according to the period-luminosity diagram

^cCorresponding to MGA99 candidate #2981

^dCorresponding to MGA99 candidate #3814

^eCorresponding to MGA99 candidate #3200

^fCorresponding to MGA99 candidate #2697

^g $M_V = -0.99$, and therefore, according to the criterium of separation between s-pCC and AC at $M_V = -1$ established in Section 5, this variable should be classified as AC. Its position in the PL diagram, however, is closer to the s-pCC locus, and therefore, given that the

separation at $M_V=-0.99$ is rather arbitrary, we tentatively classify this star as s-pCC. This is the only variable basically at the cutoff between AC and s-pCC.

Table 3. B Photometry of Cepheid variable stars

| HJD-2400000 | B | $\sigma(B)$ |
|-------------|--------|-------------|
| 7382 | | |
| 51873.61265 | 21.662 | 0.014 |
| 51410.81472 | 21.092 | 0.005 |
| 51410.82235 | 21.131 | 0.006 |
| 51410.82998 | 21.123 | 0.006 |
| 51436.73170 | 21.616 | 0.012 |
| 51550.54004 | 21.762 | 0.016 |

Note. — Table presented in its entirety in the electronic edition of the AJ only

Table 4. V Photometry of Cepheid variable stars

| HJD-2400000 | V | $\sigma(V)$ |
|-------------|--------|-------------|
| 7382 | | |
| 48979.65277 | 21.289 | 0.023 |
| 48979.66310 | 21.355 | 0.031 |
| 48979.68438 | 21.376 | 0.028 |
| 50489.53798 | 21.025 | 0.023 |
| 50489.54583 | 20.973 | 0.018 |
| 50489.55051 | 20.974 | 0.019 |

Note. — Table presented in its entirety in the electronic edition of the AJ only

Table 5. I Photometry of Cepheid variable stars

| HJD-2400000 | I | $\sigma(I)$ |
|-------------|--------|-------------|
| 7382 | | |
| 50488.56482 | 20.781 | 0.061 |
| 50489.55558 | 20.559 | 0.045 |
| 50489.56002 | 20.534 | 0.041 |
| 50489.56445 | 20.570 | 0.041 |
| 50490.54965 | 20.849 | 0.024 |
| 50490.55756 | 20.847 | 0.024 |

Note. — Table presented in its entirety in the electronic edition of the AJ only